NeuroImage 141 (2016) 326–340

Contents lists available at ScienceDirect

NeuroImage

journal homepage: www.elsevier.com/locate/ynimg

Cerebral responses to local and global auditory novelty under general anesthesia

Lynn Uhrig MD PhD [a,b], David Janssen [a], Stanislas Dehaene PhD [a,b,c,d], Béchir Jarraya MD PhD [a,b,e,f,*]

[a] CEA DRF/I2BM, NeuroSpin Center, 91191 Gif-sur-Yvette, France
[b] INSERM U992, Cognitive Neuroimaging Unit, 91191 Gif-sur-Yvette, France
[c] Collège de France, 75231 Paris, France
[d] Université Paris Sud, Université Paris-Saclay, 91405 Orsay, France
[e] Neuromodulation Unit, Department of Neurosurgery, Foch Hospital, 92150 Suresnes, France
[f] University of Versailles Saint-Quentin-en-Yvelines, Université Paris-Saclay, 78000 Versailles, France

ARTICLE INFO

Article history:
Received 1 January 2016
Accepted 3 August 2016
Available online 05 August 2016

Keywords:
Anesthesia
Sequence violation
Cortex
Thalamus
fMRI
Primate

ABSTRACT

Primate brains can detect a variety of unexpected deviations in auditory sequences. The local-global paradigm dissociates two hierarchical levels of auditory predictive coding by examining the brain responses to first-order (local) and second-order (global) sequence violations. Using the macaque model, we previously demonstrated that, in the awake state, local violations cause focal auditory responses while global violations activate a brain circuit comprising prefrontal, parietal and cingulate cortices. Here we used the same local-global auditory paradigm to clarify the encoding of the hierarchical auditory regularities in anesthetized monkeys and compared their brain responses to those obtained in the awake state as measured with fMRI. Both, propofol, a GABAA-agonist, and ketamine, an NMDA-antagonist, left intact or even enhanced the cortical response to auditory inputs. The local effect vanished during propofol anesthesia and shifted spatially during ketamine anesthesia compared with wakefulness. Under increasing levels of propofol, we observed a progressive disorganization of the global effect in prefrontal, parietal and cingulate cortices and its complete suppression under ketamine anesthesia. Anesthesia also suppressed thalamic activations to the global effect. These results suggest that anesthesia preserves initial auditory processing, but disturbs both short-term and long-term auditory predictive coding mechanisms. The disorganization of auditory novelty processing under anesthesia relates to a loss of thalamic responses to novelty and to a disruption of higher-order functional cortical networks in parietal, prefrontal and cingular cortices.

© 2016 Published by Elsevier Inc.

1. Introduction

Anesthetic agents are capable of suppressing conscious experience, verbal reportability and behavioral responsivity, partially or totally, in a reversible manner. Several molecular and cellular pharmacological mechanisms of anesthetics have been identified (Alkire et al., 2008; Franks, 2008; Uhrig et al., 2014a). Neural circuit mechanisms of anesthetics are covered in two recent reviews (Brown et al., 2010; Purdon et al., 2015). In the recent years, the cerebral consequences of anesthetic administration at the systems level have been increasingly characterized using different modalities of functional neuroimaging (reviewed in MacDonald et al., 2015). Anesthetics induce a functional disruption of large-scale cortico-cortical networks (Lee et al., 2009a; Ku et al., 2011; Lee et al., 2013), and generate slow delta and alpha oscillations in thalamo-cortical circuits (Ching et al., 2010; Cimenser et al., 2011). The functional organization of brainscale networks can also be studied by measuring spontaneous coherent fluctuations of functional magnetic resonance imaging (fMRI) signals in the brain. In awake monkeys, these fluctuations engage widely distributed default-mode networks that underlie the "intrinsic functional architecture" of the brain (Buckner et al., 2008; Mantini et al., 2011). Surprisingly, this intrinsic architecture is partially preserved even in deeply anesthetized macaques (Vincent et al., 2007). However, we recently showed by using dynamical functional connectivity measures that anesthesia decreases the repertoire of resting-state functional configurations to a limited number of states, mainly correlated to brain anatomy (Barttfeld et al., 2015).

Here, we specifically ask how anesthesia affects auditory information processing. While early sensory processing of external stimuli is preserved during anesthesia (Plourde et al., 2006; Hudetz et al., 2009; Boveroux et al., 2010), few experiments have studied how anesthesia affects the higher-order brain responses to more complex auditory stimuli (Kerssens et al., 2005; Adapa et al., 2014). Here, we use a

* Corresponding author at: Neurospin Imaging Center, Inserm, CEA Saclay, Bat 145, 91191 Gif-sur-Yvette, France.
E-mail address: bechir.jarraya@cea.fr (B. Jarraya).

http://dx.doi.org/10.1016/j.neuroimage.2016.08.004
1053-8119/© 2016 Published by Elsevier Inc.

hierarchical paradigm to evaluate the auditory processing of rule violation during anesthesia, and to test the hypothesis that anesthesia relates to a functional disruption of higher-order cortical interactions that support information integration and broadcasting (Dehaene and Changeux, 2011; Oizumi et al., 2014).

The local-global paradigm probes auditory sequence processing at first-order (local) and second-order (global) sequence violations (Bekinschtein et al., 2009). The global novelty effect activates a widely organized network that is considered as a signature of conscious processing, as validated in patients with disorders of consciousness (Faugeras et al., 2011). Using the local-global paradigm, we previously demonstrated that the macaque brain is capable of hierarchical predictive coding through a ≪macaque Global Neuronal Workspace (GNW)≫ that is homologous to the human GNW (Uhrig et al., 2014b). The GNW framework is a theoretical model which stipulates that the global availability of sensory information to widely distributed prefronto-parietal and cingulate cortical areas subtends conscious access (Dehaene et al., 1998; Dehaene and Naccache, 2001; Baars, 2005; Shanahan and Baars, 2005; Dehaene and Changeux, 2011).

Examining whether auditory responses to sounds are preserved, and which cortical stage of auditory processing is disrupted, should help dissect the functional reorganization underlying the information processing under anesthesia. Anesthetics may act through the disruption of the GNW, but they may also alter early auditory thalamo-cortical information processing. To evaluate these possibilities, we employed EEG-controlled anesthesia and fMRI in macaques presented with the local-global auditory paradigm (Bekinschtein et al., 2009). The results demonstrate, surprisingly, that anesthesia does not fully suppress the cerebral responses to second-order (global) sequence violations. Instead, an absence of cerebral activations to the global effect in parietal cortex and thalamus appears as the common denominator for anesthesia with propofol and ketamine.

2. Material and methods

2.1. Animals

Four rhesus macaques (Macaca mulatta), 1 male (monkey J) and 3 females (monkeys K, Ki and R) (5–8 kg, 8–12 years of age), were tested, 3 for each arousal state (awake: monkeys J, K and R (Uhrig et al., 2014b), moderate propofol sedation: monkeys J, K and R; deep propofol anesthesia: J, K and R; deep ketamine anesthesia: monkeys K, Ki and R). All procedures were conducted in accordance with the European convention for animal care (86-406) and the National Institutes of Health's Guide for the Care and Use of Laboratory Animals. Animal studies were approved by the institutional Ethical Committee (CETEA protocol #10-003).

2.2. "Local-global" auditory paradigm (Fig. 1)

We used an event-related auditory paradigm based on local (within trials) and global (across trials) violations of temporal regularities, as previously described (Bekinschtein et al., 2009; Wacongne et al., 2011; Uhrig et al., 2014b; Strauss et al., 2015). The paradigm was strictly identical to our previously published work with awake monkeys (Uhrig et al., 2014b). At the local level (first hierarchical level), a deviant sound is introduced after 4 identical sounds (denoted xxxxY, where x is the repeated sound and Y the deviant sound), and such trials are contrasted with sequences of 5 identical sounds (xxxxx). At the global level (second hierarchical level), a sequence of trials, called the 'global standard', is repeatedly presented (e.g. xxxxY), and then this regularity is violated by rare trials called 'global deviants' (e.g. xxxxx). Each trial comprised five consecutive sounds (50 ms duration, 150 ms stimulus onset asynchrony (SOA) between sounds, total duration of 650 ms), separated by 850 ms of silence, for a total trial duration of 1500 ms. Each series of 24 trials comprised an initial 4 habituation trials, followed by 20 post-habituation trials with 4 deviant trials (followed by at least 2 consecutive standard trials) and 16 standard trials. The sounds were presented within runs comprising a period of rest (14.4 s), followed by 5 series of 24 trials (36 s,) and at the end of each trial another period of rest (14.4 s), for a total duration of 266.4 s. Two runs used as global standard the xxxxx sequence of 5 identical sounds (either high pitched 1600 Hz or low pitched 800 Hz) and two other runs used the xxxxY sequence (same pitch, with the final sound swapped). All four run types were presented in random order and comprised both a local regularity (the fifth sound could be different or identical to previous sounds) and a global regularity (one of the series of sounds was less frequent than the other). Auditory stimuli were presented using the E-prime software (E-Studio 1.0, Psychology Software Tools; http://www.pstnet.com) and delivered using MR-compatible headphones (MR CONFON, Germany).

2.3. Anesthesia protocols

Monkeys received anesthesia with either propofol or ketamine.

For propofol anesthesia (Barttfeld et al., 2015), three monkeys (monkey K, R and J) were scanned in different scanning sessions under two different levels of anesthesia, either moderate propofol sedation or deep propofol anesthesia corresponding to a level of general anesthesia. The levels of anesthesia were targeted using both a behavioral monkey sedation scale (Table 1) and electroencephalography (EEG).

First the awake monkeys were trained for i.v. propofol injection in the saphenous vein for induction of anesthesia (propofol bolus, 5–7.5 mg/kg i.v.; Fresenius Kabi, France). Induction of anesthesia was followed by a target-controlled infusion (TCI) (Alaris PK Syringe pump, CareFusion, CA, USA) of propofol based on the 'Paedfusor' pharmacokinetic model (Absalom and Kenny, 2005). The level of TCI for the propofol infusion was adapted to the behavior score and the EEG of each individual monkey on each fMRI session. Based on the behavior and the EEG, the TCI for the moderate propofol sedation state was 3.7–4.6 μg/ml (monkey J 3.7 μg/ml; monkey K: 4–4.6 μg/ml; monkey R: 3.7–3.9 μg/ml) and for the deep propofol anesthesia state 5.8–7.2 μg/ml (monkey J 5.8–5.9 μg/ml; monkey K: 6.5–7.2 μg/ml; monkey R 5.8 μg/ml).

For ketamine anesthesia, three animals (monkeys K, Ki and R) were scanned at a deep level of ketamine anesthesia, defined using the monkey sedation scale and EEG. For ketamine anesthesia induction, monkeys received an intramuscular (i.m.) injection of ketamine (20 mg/kg i.m., Virbac, France). To maintain a deep ketamine anesthesia state, induction of anesthesia was followed by a continuous intravenous infusion of ketamine (15–16 mg/kg/h i.v.; monkey K 16 mg/kg/h; monkey Ki 16 mg/kg/h; monkey R 15 mg/kg/h) based on the behavior scale and the EEG. Atropine (0.02 mg/kg i.m., Aguettant, France) was injected 10 min before ketamine induction, to reduce salivary and bronchial secretions. To avoid artifacts related to potential movements during MRI acquisition, during the moderate propofol sedation and deep ketamine anesthesia, a muscle blocking agent was co-administered when the monkey was inside the scanner (cisatracrium, 0.15 mg/kg bolus i.v. followed by continuous i.v. infusion at a rate of 0.18 mg/kg/h, GlaxoSmithKline, France) (Barttfeld et al., 2015). In all anesthesia conditions, monkeys were intubated and ventilated as previously described (Barttfeld et al., 2015). Heart rate, non-invasive blood pressure (systolic/diastolic/mean), oxygen saturation (SpO2), respiratory rate, end-tidal CO2 (EtCO2), cutaneous temperature was monitored (Maglife, Schiller, France) and recorded online (Schiller, France). I.v. hydration was ensured by a mixture of normal saline (0.9%) and 5% glucose (250 ml of normal saline with 100 ml of 5% glucose; rate of 10 ml/kg/h).

2.4. Clinical arousal scale for monkeys (Table 1)

The levels of arousal were defined on a behavioral scale, based on spontaneous movements and the response to juice presentation, shaking/prodding, toe pinch and corneal reflex (Table 1). Such behavioral

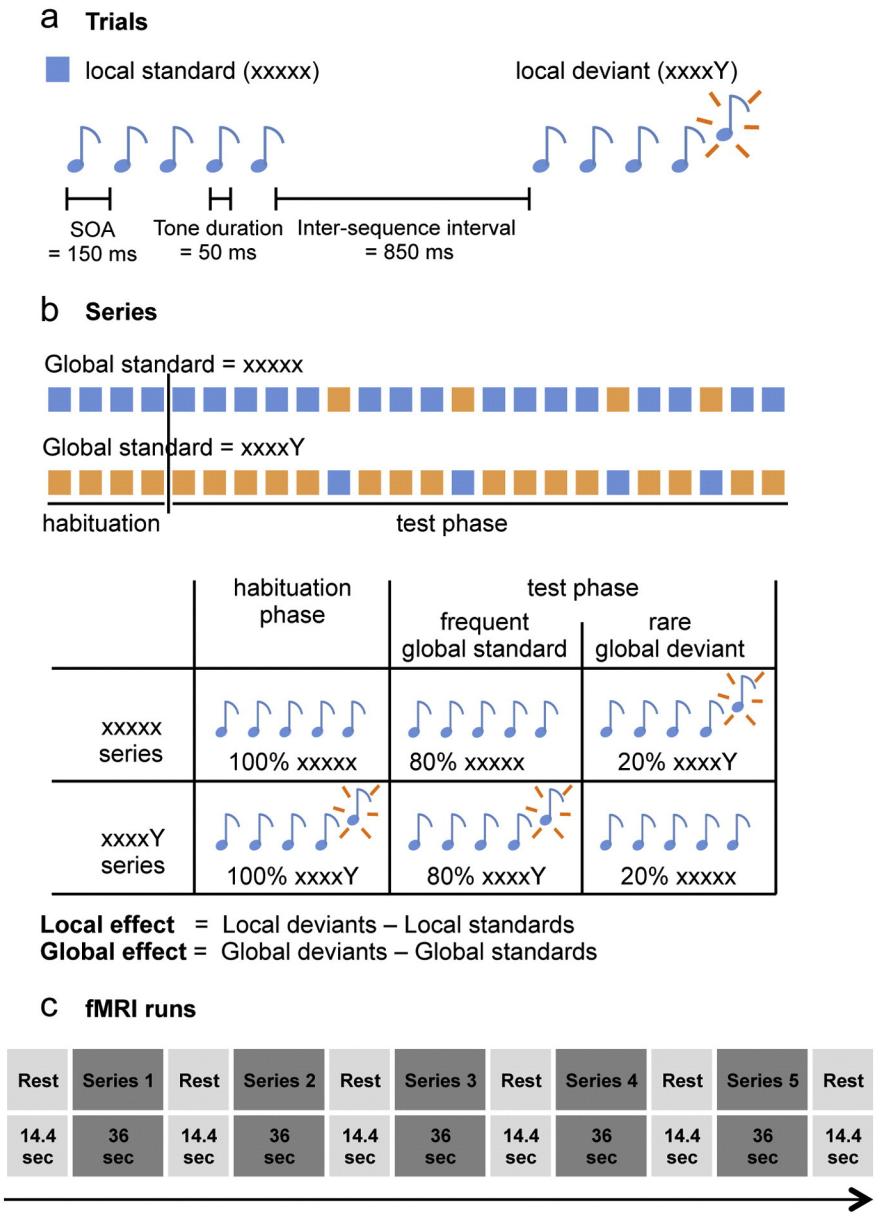

Fig. 1. 'Local/global' paradigm. a, Trial: short auditory sequences containing either 5 identical sounds (local standard, denoted as xxxxx), or 4 identical sounds followed by a distinct one (local deviant, denoted as xxxxY). b, Series: 24 trials with an initial 4 habituation trials, followed by 20 test-phase trials; 4 deviant trial and 16 standard trials. Stimuli presentation, one sequence served as the global standard and another as the global deviant. c, Run: initial period of rest (14.4 s), 5 series of 24 trials (36 s), period of rest (14.4 s) at the end of each trial, total duration of the run of 266.4 s.
Adapted from Uhrig et al. (2014b).

testing was performed both before the animal was paralyzed, at the beginning of the fMRI session, and again at the end of the fMRI session once the animal was no longer paralyzed. The parts of the behavioral assessment were performed in the same order: first the response to juice presentation, followed by spontaneous movements, then shaking/prodding, toe pinch and at the end the corneal reflex (with a wisp of cotton).

2.5. Electroencephalography (Table 1)

We acquired scalp EEG using an MR-compatible system and custom-built caps as previously described (Barttfeld et al., 2015). EEG scalp recordings were performed using a customized EEG cap (EasyCap, 13 channels, Fp1, Fp2, F3, F4, T3, T4, P3, P4, O1, O2, Oz, reference electrode, ground electrode), an MR amplifier (BrainAmp, Brain Products, Germany) and the Vision Recorder software (Brain Products). Parameters were as follow: sampling rate, 5000 per channel; common reference electrode, impedance, <20 MΩ; band-pass filtered 0.01 Hz < f < 500 Hz during collection. We applied an EEG gel to obtain low impedances (One Step EEG gel, Germany). EEG-fMRI gradient artifacts were removed before analysis with BrainVision Analyzer 2 software (Brain Products). EEG recordings before fMRI acquisitions, gave EEG windows free of gradient artifacts (Supplementary Fig. 10).

For propofol, 5 levels were defined as follows: level 1, awake state, posterior alpha waves (eyes closed) and anterior beta waves; level 2, light propofol sedation, increased amplitude of alpha waves and anterior diffusion of alpha waves; level 3, moderate propofol sedation, diffuse and wide alpha waves, and anterior theta waves (Feshchenko et al., 2004); level 4, deep propofol general anesthesia, diffuse delta waves, waves of low amplitude (Steriade et al., 1993; Murphy et al., 2011) and anterior alpha waves (10 Hz) (Purdon et al., 2013); level 5, very deep anesthesia (deeper than the level of general anesthesia), burst suppression. For ketamine, sedation levels were defined as follow:

Table 1
Arousal scale.

Scale	Arousal	Monkey sedation scale						
		Behavior					EEG	
		Juice presentation	Spontaneous movements	Shaking/prodding	Toe pinch	Corneal reflex	Propofol	Ketamine
1	Alert/awake	+	+	+	+	+	Posterior alpha waves, anterior beta waves	Posterior alpha waves, anterior beta waves
2	Light sedation	−	+	+	+	+	Increased amplitude of alpha waves, anterior diffusion of alpha waves	Loss of alpha rhythm, decrease of amplitude
3	Moderate sedation	−	−	±	+	+	Diffuse and wide alpha waves, anterior theta waves	Persistent rhythmic theta activity, increasing amplitude, beta activity of low amplitude
4	Deep anesthesia/general anesthesia	−	−	−	−	−	Diffuse delta waves, waves of low amplitude, anterior alpha waves	Intermittent polymorphic delta activity of large amplitude, superimposed beta activity of low amplitude, increase in gamma power

Arousal scale based on the monkey sedation scale (behavior) and EEG for propofol, respectively ketamine anesthesia Note: Response to juice presentation: the experimenter presents a syringe with juice/water. (+) if the monkey drinks, (−) if the monkey fails to drink. Spontaneous movements: (+) if the monkey exhibits spontaneous movements, (−) if spontaneous movements are absent. Shaking/prodding: (+) if the monkey exhibits a response (body movement, eye blinking, eye opening, cardiac rate change) on Shaking/prodding, (−) if there is no response. Toe pinch: (+) if the monkey exhibits a response (body movement, eye blinking, eye opening, cardiac rate change) to toe pinch, (−) if there is no response. Corneal reflex: (+) if the corneal reflex is present, (−) if the corneal reflex is absent.

level 1, awake state, posterior alpha waves (eyes closed) and anterior beta waves; level 2, light ketamine sedation, loss of alpha rhythm with a decrease of amplitude (Schuttler et al., 1987); level 3, moderate ketamine sedation, persistent rhythmic θ activity (4–6 Hz) with increasing amplitude, and fast β activity (14–20 Hz) of low amplitude (Schuttler et al., 1987); level 4, deep ketamine anesthesia, intermittent polymorphic δ activity (0.5–2 Hz) of large amplitude, with superimposed β activity (14–20 Hz) of low amplitude (Schuttler et al., 1987), increase in γ power (30–100 Hz) (Pinault, 2008).

2.6. fMRI data acquisition

Monkeys were scanned on a 3T horizontal scanner (Siemens Tim Trio, Erlanger, Germany) with a custom-built single transmit-receiver surface coil. Monocrystalline iron oxide nanoparticle (MION, Feraheme, AMAG Pharmaceuticals, MA; 10 mg/kg, i.v.), was injected before each scanning session (Vanduffel, 2001). Each functional scan (time series) consisted of 111 gradient-echo echo-planar whole-brain images (TR 2400 ms, TE 20 ms and 1.5 mm3 voxel size). Animals were positioned in the sphinx position inside the MR scanner for the anesthesia experiments. To compare the anesthesia states with the awake state, we used data acquired in awake monkeys from a previous experiment (Uhrig et al., 2014b). For the awake experiment (Uhrig et al., 2014b), monkeys were implanted with an MR-compatible headpost and trained to sat in a sphinx position in a primate chair with their head fixed and fixate a red dot inside a "mock" MR bore before being scanned.

In total, 829 runs were analyzed for the experiment: 148 runs for the awake state (Monkey J: 88 runs, 6 fMRI session; Monkey K: 35 runs, 6 fMRI sessions; Monkey R: 25 runs, 3 fMRI sessions), 227 runs for the moderate propofol sedation (Monkey J: 32 runs, 2 fMRI sessions; Monkey K: 135 runs, 7 fMRI sessions; Monkey R: 60 runs, 8 fMRI sessions), 230 runs for the deep propofol anesthesia (Monkey J: 56 runs, 6 fMRI sessions; Monkey K: 89 runs, 5 fMRI sessions; Monkey R: 85 runs, 6 fMRI sessions) and 224 runs for deep ketamine anesthesia (Monkey K: 81 runs, 5 fMRI sessions; Monkey Ki: 52 runs, 5 fMRI sessions; Monkey R: 91 runs, 5 fMRI sessions).

2.7. fMRI analyses

Functional images were reoriented, realigned, resampled (1 mm isotropic), smoothed (Gaussian kernel, 3 mm full width at half maximum) and rigidly co-registered to the anatomical template of the monkey MNI space (Frey et al., 2011) using custom-made scripts (Uhrig et al., 2014b). Whole brain data were displayed using Caret software (version 5.61, brainvis.wustl.edu/wiki/index.php/Caret:About).

829 runs were analyzed for the experiment with a two-level analysis (SPM5 software, Wellcome Department of Cognitive Neurology, London, UK; Matlab, MathWorks, MA):

2.7.1. Whole-brain individual analyses

For each subject, the activation time series was modeled, within each fMRI run, using regressors obtained by convolution of the experimental conditions with the canonical hemodynamic response function for MION, and its time derivative (Uhrig et al., 2014b).

2.7.2. Whole-brain group analyses

For each subject and each fMRI session, the first-level SPM model produced a beta weight image of activation for each condition relative to rest (percentage of the whole-brain signal). Images were then inserted into several second-level whole-brain ANOVAs (Uhrig et al., 2014b). The contrasts were: activation to all sounds (habituation, frequent and rare sequences) relative to rest; global standard sequences relative to rest; global deviant sequences relative to rest; local effect (local deviant minus local standard sequences); and global effect (rare minus frequent sequences). For all of the whole-brain analyses a threshold of $p < 0.001$ uncorrected was applied at the voxel level, and we report only regions where such voxels grouped together to form a contiguous cluster whose extent was significant at $p < 0.05$, corrected for multiple comparisons across the brain volume (False Detection Rate, FDR, $p < 0.05$). t-Test values and pFDR (FDR corrected) values are reported at local maxima of each significantly activated region.

2.7.3. Plots

Plots were generated by extracting the beta weight of SPM regressions of individual subject data with the hemodynamic functions of the appropriate stimulus category. The mean and the standard error of these beta weights were plotted. Activity profiles, plotting the % signal change, for the different experimental conditions, were computed on ROIs of 7 voxels in size centered on the most significant voxel.

2.7.4. Event related functional correlation using psychophysiological interaction (PPI)

To determine the effect of novelty (local or global auditory violation) on the functional correlation between the primary auditory cortex (A1) and the remaining brain areas, a psychophysiological interaction (PPI) analyses (Friston et al., 1997) was conducted using SPM5 across all

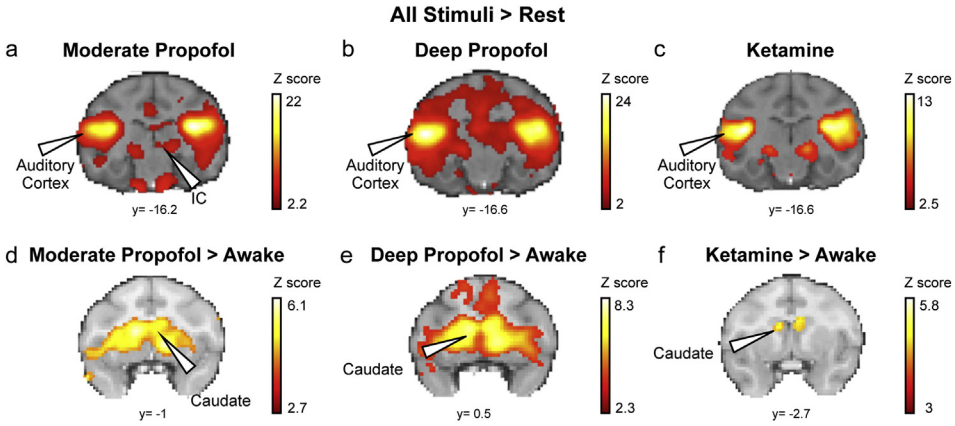

Fig. 2. fMRI activations to all sounds relative to rest. fMRI activations to all sounds relative to rest (a–c) under moderate propofol sedation, deep propofol anesthesia and deep ketamine anesthesia. Panels d–f show the corresponding comparisons between the awake state and moderate propofol sedation, deep propofol anesthesia and deep ketamine anesthesia. SPM maps for all sounds overlying coronal T1-weighted images from the macaque MNI atlas. y, level of coronal section relative to the bregma in the Paxinos atlas. Group analysis, $p < 0.05$, FDR corrected. a, all sounds relative to rest for moderate propofol sedation; b, all sounds relative to rest for deep propofol anesthesia; c, all sounds relative to rest for deep ketamine anesthesia; d, stronger activations for all sounds during moderate propofol sedation compared to the awake state; e, stronger activations for all sounds during deep propofol anesthesia compared to awake state; f, stronger activations for all sounds during deep anesthesia sedation compared to the awake state; IC, inferior colliculus; Caudate, Caudate nucleus.

sessions (Uhrig et al., 2014b) from the four monkeys. For the PPI analysis, the residual of the above first-level model was extracted in the primary auditory regions that were activated by sounds. This residual, together with its point-by-point multiplication with the prior regressors for habituation, global standards and global deviants, was then entered as additional regressors in a novel first-level model. In the end, their beta weights were submitted to the same second-level analysis as above, with the same contrasts allowing us to determine which areas increased their functional correlation to auditory cortex during, e.g. global deviants relative to global standards. The statistical threshold was set at $p < 0.05$ (FDR corrected). We report t-test values and pFDR (FDR corrected) values at local maxima of each significantly activated region.

2.7.5. Comparison between arousal states

For each monkey, beta weights of activations relative to rest for each session and each arousal state (awake, moderate propofol sedation, deep propofol anesthesia, deep ketamine anesthesia) were entered into several second-level whole-brain ANOVAs. The contrasts that we studied were: all sounds, frequent sounds, rare sounds, local effect, global effect; interacting with contrasts for awake vs moderate propofol sedation; awake vs deep propofol anesthesia; awake vs deep ketamine anesthesia; moderate propofol vs deep ketamine anesthesia; and deep propofol vs deep ketamine anesthesia. For all of these whole-brain analyses we used the same thresholds as above (voxelwise $p < 0.001$, uncorrected, and clusterwise $p < 0.05$, FDR-corrected).

3. Results

Physiological parameters related to general hemodynamic, ventilation and temperature were kept constant during each experiment (Supplementary Table 1). In all sessions and in all animals, the moderate sedation level and deep anesthesia level, as defined by the monkey sedation scale (Table 1), corresponded, respectively to levels 3 and 4 as defined by the EEG traces for each drug (propofol or ketamine) (Supplementary Figs. 10–11).

We found consistent patterns of fMRI activations in the monkeys, and therefore report group results after normalization (for individual results, see Fig. 6, Tables 4–5, Supplementary Figs. 5–9 and Supplementary Tables for individual monkeys).

3.1. fMRI activation to auditory stimuli persists and is even enhanced under propofol anesthesia (Fig. 2, Supplementary Table 2)

We first examined the group activations relative to rest. During moderate propofol sedation, pooling over all stimuli, we observed bilateral fMRI activations within the bilateral auditory cortex including core

Table 2
fMRI activations for the local novelty effect.

		Area	Awake		Deep ketamine anesthesia	
			t value	p value	t value	p value
Local novelty effect	Left	Auditory cortex	5.15	pFDR = 0.005	n.s.	n.s.
	Right	Auditory cortex	3.59	puncorrected = 1.95 × 10−4	n.s.	n.s.
	Left	MGN	5.5	pFDR = 0.002	n.s.	n.s.
	Right	MGN	3.95	pFDR = 0.025	n.s.	n.s.
		ACC	3.42	pFDR = 0.048	n.s.	n.s.
	Left	Parietal cortex	n.s.	n.s.	4.62	pFDR = 0.012
	Right	Parietal cortex	n.s.	n.s.	5.14	pFDR = 0.012
		Area 23	n.s.	n.s.	4.4	pFDR = 0.012
	Left	Medial superior temporal area	4.73	pFDR = 0.01	4.52	pFDR = 0.012
	Right	Medial superior temporal area	4.63	pFDR = 0.01	n.s.	n.s.
	Left	Putamen	4.63	pFDR = 0.010	4.48	pFDR = 0.012
	Left	Caudate	3.72	pFDR = 0.033		
	Right	Caudate	4.43	pFDR = 0,012	3.89	pFDR = 0.017
	Right	Area V4	4.27	pFDR = 0.015	4.25	pFDR = 0.013
		Dorsal thalamus	4.09	pFDR = 0.020	4.33	pFDR = 0.0012

fMRI activations for the local novelty effect in the awake state and under deep ketamine anesthesia. We found no significant activations for the local novelty effect during moderate propofol sedation and deep propofol anesthesia. MGN, medial geniculate nucleus; ACC, anterior cingulate cortex. p values refer to FDR correction, unless stated. Uncorr, uncorrected. n.s., not significant.

Table 3
fMRI activations for the global novelty effect.

		Area	Awake		Moderate propofol sedation		Deep propofol anesthesia	
			t value	p value	t value	p value	t value	p value
Global novelty effect	Left	Auditory cortex	4.14	pFDR = 0.017	6.55	pFDR = 0 puncorrected = $2.2 \times 10-13$	8.64	pFDR = 0 puncorrected = $4.4 \times 10-16$
	Right	Auditory cortex	4.51	pFDR = 0.008	8.05	pFDR = 0 puncorrected = $1.4 \times 10-12$	4.83	pFDR = 0.001
	Left	MGN	n.s.	n.s.	3.49	pFDR = 0.012	n.s.	n.s.
	Right	MGN	n.s.	n.s.	3.43	pFDR = 0.015	n.s.	n.s.
		ACC	3.71	pFDR = 0,038	5.26	pFDR = 0 puncorrected = $1.1 \times 10-7$	4.01	pFDR = 0.002
	Left	Prefrontal cortex area 46	n.s.	n.s.	4.61	pFDR = 0 puncorrected = $2.7 \times 10-6$	3.85	pFDR = 0.002
	Right	Prefrontal cortex area 46	n.s.	n.s.	3.67	pFDR = 0.007	3.25	pFDR = 0.011
	Left	Prefrontal area 8A	5.31	pFDR = 0.003	4.61	pFDR = 0 puncorrected = $2.7 \times 10-6$	3.6	pFDR = 0.005
	Right	Prefrontal area 8A	4.79	pFDR = 0.006	3.67	pFDR = 0.007	4.27	pFDR = 0 puncorrected = $1.6 \times 10-5$
	Left	Premotor area 6V	5.31	pFDR = 0.003	n.s.	n.s.	3.73	pFDR = 0.003
	Right	Premotor area 6V	4.38	pFDR = 0,011	n.s.	n.s.	3.68	pFDR = 0.004
	Left	Parietal cortex (VIP)	4.97	pFDR = 0.005	n.s.	n.s.	n.s.	n.s.
	Left	Area TPt	5.09	pFDR = 0.004	n.s.	n.s.	n.s.	n.s.
	Left	Putamen	n.s.	n.s.	3.46	pFDR = 0.014	4.38	pFDR = 0 puncorrected = $1.6 \times 10-5$
	Right	Putamen	3.91	pFDR = 0.025	3.29	pFDR = 0.021	4.84	pFDR = 0 puncorrected = $1.6 \times 10-5$
	Left	Caudate	n.s.	n.s.	n.s.	n.s.	4.86	pFDR = 0 puncorrected = $1.6 \times 10-5$
	Right	Caudate	n.s.	n.s.	3.14	pFDR = 0.029	4.8	pFDR = 0 puncorrected = $1.6 \times 10-5$
	Left	Area V4	n.s.	n.s.	n.s.	n.s.	3.87	pFDR = 0.002
	Right	Area V4	n.s.	n.s.	n.s.	n.s.	6.01	pFDR = 0 puncorrected = $1.9 \times 10-7$

fMRI activations for the global novelty effect in the awake state, under moderate propofol sedation and under deep propofol anesthesia. We found no significant activations for the global novelty effect during deep ketamine anesthesia. MGN, medial geniculate nucleus; ACC, anterior cingulate cortex. p values refer to FDR correction, unless stated. Uncorr, uncorrected. n.s., not significant.

(A1, R), belt and parabelt regions, as well as in medial geniculate nucleus (auditory thalamus), inferior colliculus (IC), prefrontal area 46, anterior cingulate cortex, hippocampus, caudate, premotor area 6V (Fig. 2, Supplementary Table 2). During the test period, global standard sequences, which were frequent and predictable, caused a detectable activation relative to rest only in auditory cortex (A1) and inferior colliculus (Supplementary Table 3). The rare global deviant sequences relative to rest activated bilateral auditory cortex (core, belt and parabelt regions), inferior colliculus, anterior cingulate cortex, prefrontal area 46, prefrontal area 8A/45, left premotor area 6V, putamen, and left caudate (Supplementary Fig. 1a, Supplementary Table 4).

When comparing to our previous published data on awake monkeys (Uhrig et al., 2014b), we found no stronger activations to all sounds in the awake state compared to moderate propofol sedation. On the contrary, surprisingly, many areas showed stronger activation in the moderate propofol state compared to the awake state: auditory cortex

Table 4
fMRI activations for the global novelty effect, individual results.

		Area	Monkey K		Monkey R		Monkey J	
			t value	p value	t value	p value	t value	p value
Global novelty effect	Left	Auditory cortex	t = 7.58	pFDR = $2 \times 10-9$	t = 5.05	pFDR = 0.005 puncorrected = $8.6 \times 10-7$	t = 4.32	puncorrected = $3.2 \times 10-5$
	Right	Auditory cortex	t = 8.28	pFDR = $2.5 \times 10-10$	t = 5.72	pFDR = 0.002 puncorrected = $4.6 \times 10-8$	t = 4.33	puncorrected = $3.2 \times 10-5$
	Left	MGN	t = 3.57	pFDR = 0.012	n.s.	n.s.	n.s.	n.s.
	Right	MGN	n.s.	n.s.	n.s.	n.s.	n.s.	n.s.
		ACC	t = 4.27	pFDR = 0.001	t = 3.49	puncorrected = $3.4 \times 10-4$	t = 4.16	puncorrected = $6 \times 10-5$
	Left	Prefrontal cortex area 46	t = 4.53	pFDR = 0.001	n.s.	n.s.	n.s.	n.s.
	Right	Prefrontal cortex area 46	n.s.	n.s.	n.s.	n.s.	n.s.	n.s.
	Left	prefrontal area 8A	t = 3.73	pFDR = 0.007	t = 3.16	puncorrected = 0.001	t = 4.37	puncorrected = $2.7 \times 10-5$
	Right	Prefrontal area 8A	t = 3.76	pFDR = 0.007	t = 3.15	puncorrected = 0.001	t = 3.88	puncorrected = $1.4 \times 10-4$
	Left	Premotor area 6V	n.s.	n.s.	t = 3.56	pFDR = 0.049 puncorrected = $2.8 \times 10-4$	n.s.	n.s.
	Right	Premotor area 6V	n.s.	n.s.	t = 3.46	puncorrected = $3.9 \times 10-4$	t = 3.36	puncorrected = 0.001
	Left	Area TPt	n.s.	n.s.			n.s.	n.s.
	Left	Putamen	t = 3.21	pFDR = 0.032	t = 3.27	puncorrected = 0.001	n.s.	n.s.
	Right	Putamen	n.s.	n.s.	n.s.	n.s.	n.s.	n.s.
	Left	Caudate	n.s.	n.s.	n.s.	n.s.	n.s.	n.s.
	Right	Caudate	n.s.	n.s.	n.s.	n.s.	t = 4.26	puncorrected = $4 \times 10-5$

Individual results for fMRI activations for the global novelty effect in the awake state, under moderate propofol sedation. MGN, medial geniculate nucleus; ACC, anterior cingulate cortex. Uncorr, uncorrected. n.s., not significant.

Table 5
fMRI activations for the global novelty effect, individual results.

		Area	Monkey K		Monkey R		Monkey J	
			t value	p value	t value	p value	t value	p value
Global novelty effect	Left	Auditory cortex	t = 6.36	pFDR = 2.4 × 10−5	t = 6.94	pFDR = 2.5 × 10−6	t = 3.69	puncorrected = 1.8 × 10−4
	Right	Auditory cortex	t = 6.44	pFDR = 2.4 × 10−5	t = 6.3	pFDR = 3.4 × 10−6	t = 3.53	puncorrected = 3.1 × 10−4
		ACC	t = 3.92	pFDR = 0.006	t = 4.37	pFDR = 0.001	n.s.	n.s.
	Left	Prefrontal cortex area 46	t = 3.68	pFDR = 0.010	t = 3.69	pFDR = 0.005	n.s.	n.s.
	Right	Prefrontal cortex area 46	t = 4.36	pFDR = 0.002	n.s.		t = 3.46	puncorrected = 4 × 10−4
	Left	Prefrontal area 8A	n.s.	n.s.	t = 4.96	pFDR = 2.1 × 10−4	t = 3.93	puncorrected = 7.6 × 10−5
	Right	Prefrontal area 8A	t = 3.64	pFDR = 0.011	t = 6.68	pFDR = 2.8 × 10−6	n.s.	n.s.
	Left	Premotor area 6V	t = 3.68	pFDR = 0.011	t = 4.3	pFDR = 0.001	n.s.	n.s.
	Right	Premotor area 6V	n.s.	n.s.	t = 3.68	pFDR = 0.005	t = 3.5	puncorrected = 3.4 × 10−4
	Left	Area TPt	n.s.	n.s.	n.s.	n.s.	n.s.	n.s.
	Left	Putamen	t = 4.7	pFDR = 0.001	t = 4.31	puncorrected = 0.001	n.s.	n.s.
	Right	Putamen	n.s.	n.s.	n.s.	n.s.	t = 5.1	puncorrected = 7.7 × 10−7
	Left	Caudate	t = 4.45	pFDR = 0.002	t = 3.61	pFDR = 0.006	n.s.	n.s.
	Right	Caudate	t = 3.75	pFDR = 0.009	t = 3.65	pFDR = 0.005	t = 3.86	puncorrected = 3.7 × 10−5
	Left	Area V4	n.s.	n.s.	t = 3.95	pFDR = 0.003	t = 4.23	puncorrected = 2.5 × 10−5
	Right	Area V4	t = 3.21	pFDR = 0.025	t = 4.4	pFDR = 0.001	t = 3.58	puncorrected = 2.6 × 10−4

Individual results for fMRI activations for the global novelty effect in the awake state, under deep propofol anesthesia. MGN, medial geniculate nucleus; ACC, anterior cingulate cortex. Uncorr, uncorrected. n.s., not significant.

including core (A1, R), belt and parabelt regions, anterior cingulate cortex, prefrontal area 46, caudate and putamen (Fig. 2d). No differences were found for global standard sequences, but during the test period, rare global deviant sequences relative to rest, caused a stronger activation in the moderate propofol sedation compared to the awake state in auditory cortex, anterior cingulate, putamen, and caudate. This result therefore suggests, not only that a subset of areas of the monkey brain continue to respond to sounds, but that they are partially released from inhibition and respond even stronger during sedation. Conversely, however, we did find several areas where the rare global deviant sequences, relative to rest, caused a stronger activation in the awake state compared to moderate propofol sedation (Supplementary Fig. 1d, g; Supplementary Table 4). These regions (anterior cingulate, thalamus parafascicular nucleus, right prefrontal area 8A, premotor area 6V, left parietal cortex, hippocampus and cerebellar dentate nuclei) are good candidates for a disruption effect due to general anesthesia.

It could be argued that the finding of preserved or even amplified activation to sound in several cortical and subcortical regions could be due to the insufficient level of propofol sedation. However, we replicated these results during deep propofol anesthesia. Pooling over all auditory stimuli relative to rest (Fig. 2b), we again found bilateral fMRI activations within the auditory cortex including core (A1, R), belt and parabelt regions, medial geniculate nucleus (auditory thalamus), inferior colliculus, anterior cingulate, premotor area 6V, prefrontal cortex area 46 and caudate. The vast majority of these regions again showed a stronger activation in the deep propofol state compared to the awake state (auditory cortex, anterior cingulate, prefrontal area 46, caudate, putamen) (Fig. 2e). Direct comparison showed that several areas increased their activation to auditory stimuli from moderate to deep propofol: auditory cortex, anterior cingulate cortex and caudate (Supplementary Table 11).

During the test period, under deep propofol anesthesia, global standard sequences, which were frequent and predictable, caused a detectable activation relative to rest only in auditory cortex (A1) and inferior colliculus (Supplementary Table 3). However, the rare global deviant sequences relative to rest activated auditory cortex (core, belt and parabelt regions), inferior colliculus, anterior cingulate, prefrontal area 46 and 8A, premotor area 6V, putamen and caudate (Supplementary Fig. 1b). Again, in the majority of these regions, the rare global deviant sequences relative to rest caused a stronger activation during deep propofol sedation compared to the awake state or to moderate propofol sedation. Still, we again identify a subset of regions whose auditory activity was disrupted during deep sedation: thalamus parafascicular nucleus, right prefrontal area 8A, premotor area 6V, parietal cortex (ventral intraparietal area, VIP), hippocampus and cerebellar dentate nuclei (Supplementary Fig. 1e, h).

3.2. Auditory activation persists under deep ketamine anesthesia (Fig. 2, Supplementary Table 2)

Propofol, a GABAA-agonist, is known to yield paradoxical enhancements of brain activity that include a strong increase in bilateral anterior

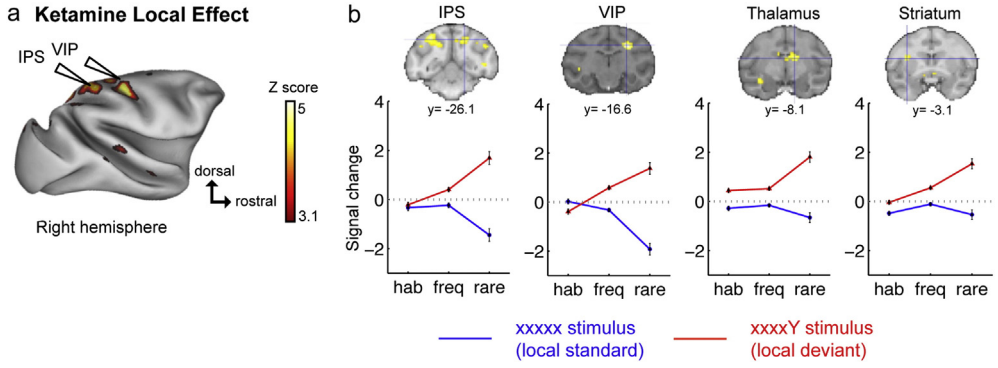

Fig. 3. Local novelty effect under anesthesia. a, Activation maps for the local novelty effect (local deviants minus local standards = (xxxxx rare + xxxxY frequent) − (xxxxx frequent + xxxxY rare)) under ketamine anesthesia. b, fMRI signal change in areas responsive to local novelty (blue cross on SPM maps) under ketamine anesthesia. Plots show signal change for habituation (hab), frequent (freq) and rare stimuli. y, level of coronal section relative to the bregma in the Paxinos atlas. Group analysis, $p < 0.05$, FDR corrected. We found no significant activations for the local novelty effect during moderate propofol sedation and deep propofol anesthesia. IPS, intraparietal sulcus; VIP, ventral intraparietal area. (For interpretation of the references to colour in this figure legend, the reader is referred to the web version of this article.)

alpha waves (Purdon et al., 2013). Thus, we probed the generality of the above results by replicating our study with a second anesthetic drug, ketamine, a NMDA-antagonist. Again, ketamine anesthesia did not result in a complete cessation of auditory activity. Pooling over all stimuli relative to rest (Fig. 2c), we still observed bilateral fMRI activations to sounds within the auditory cortex, including core (A1, R), belt and parabelt regions, the subcortical auditory pathways (medial geniculate nucleus and inferior colliculus), as well as anterior cingulate cortex, prefrontal area 46, putamen and thalamus (parafascicular nucleus). As with propofol, these activation were actually stronger in deep ketamine anesthesia compared to the awake state in the core auditory cortex (A1), anterior cingulate cortex (areas 24, 32), prefrontal area 46, caudate, putamen, and area 31 (Fig. 2f).

During ketamine anesthesia, global standard sequences caused detectable activation relative to rest in auditory cortex, medial geniculate nucleus (auditory thalamus) and anterior cingulate cortex (Supplementary Table 3). These activations were no different from the awake state. Rare global deviant sequences relative to rest, on the other hand, activated bilaterally, not only auditory cortex (core, belt and parabelt regions), inferior colliculus and medial geniculate nucleus (auditory thalamus), but also the hippocampus, prefrontal area 46, putamen, area 23/31 and anterior cingulate cortex (Supplementary Fig. 1c, Supplementary Table 4). These activations were however reduced relative to the awake state in auditory cortex (core, belt and parabelt regions), anterior cingulate, globus pallidus, thalamus (parafascicular nucleus) prefrontal area 8A, premotor area 6V, ventral intraparietal area VIP, left temporoparietal area TPt, hippocampus and cerebellar dentate nuclei (Supplementary Fig. 1f, i). The only regions showing an increased response in deep ketamine anesthesia compared to the awake state were anterior cingulate cortex and putamen.

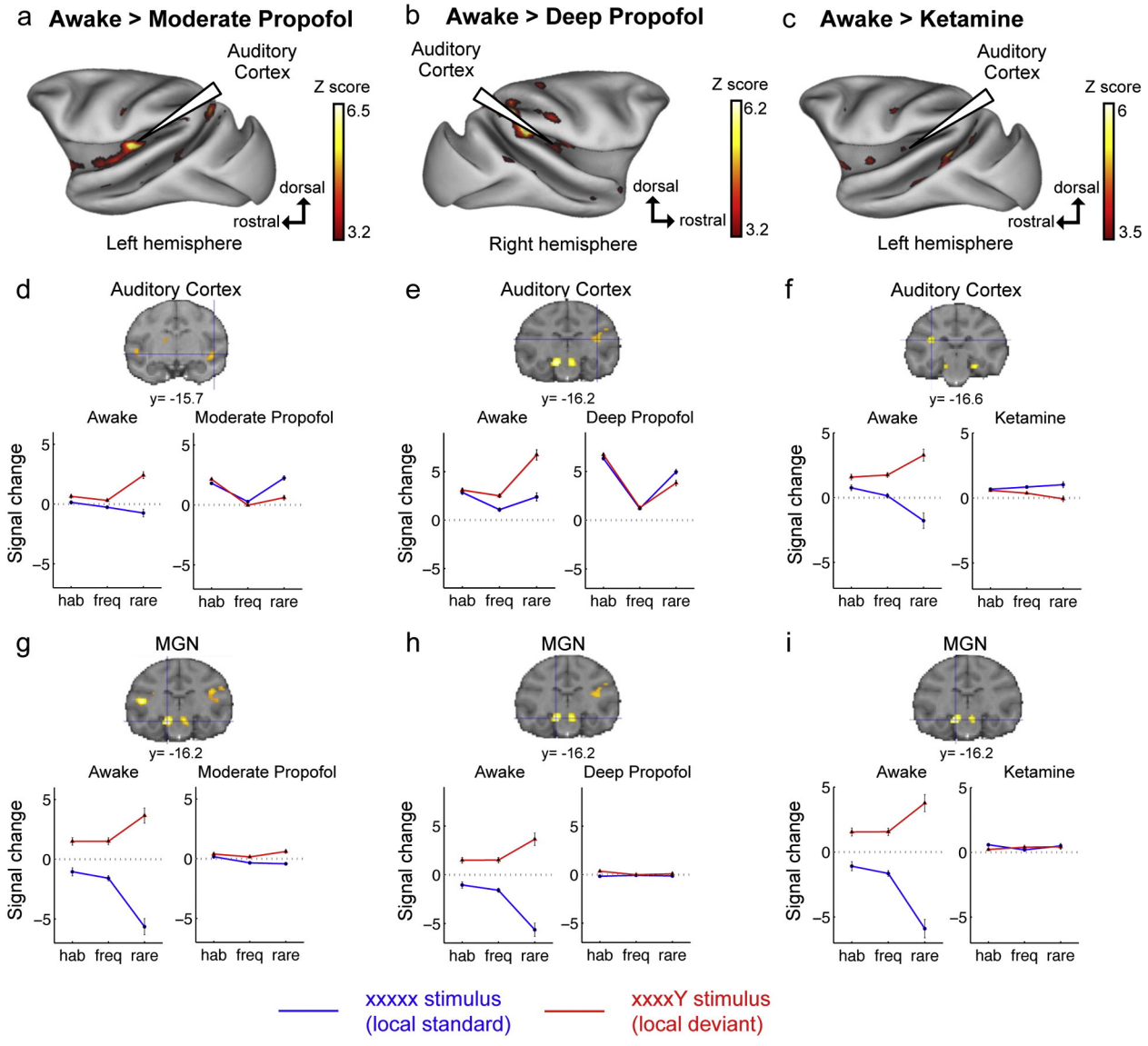

Fig. 4. Comparison between the awake state and anesthesia states for the local novelty effect. a, Activation map for local novelty effect (local deviants minus local standards) showing stronger activations in the awake state compared to moderate propofol sedation; b, Activation map for local novelty effect showing stronger activations in the awake state compared to deep propofol anesthesia; c, Activation map for local novelty effect with stronger activations in the awake state compared to deep ketamine anesthesia. Group analysis, $p < 0.05$, FDR corrected. d, g fMRI signal change in areas responsive to local novelty effect (blue cross on SPM maps) in the awake state and under moderate propofol sedation. e, h fMRI signal change in areas responsive to local novelty effect (blue cross on SPM maps) in the awake state and under deep propofol anesthesia. f, i, fMRI signal change in areas responsive to local novelty effect (blue cross on SPM maps) in the awake state and under deep ketamine anesthesia. Plots show signal change for habituation (hab), frequent (freq) and rare stimuli in the auditory cortex and medial geniculate nucleus. y, level of coronal section relative to the bregma in the Paxinos atlas. MGN, medial geniculate nucleus. (For interpretation of the references to colour in this figure legend, the reader is referred to the web version of this article.)

3.3. Local and Global novelties are partially disrupted by propofol anesthesia (Tables 2, 3, 4, 5)

While brain responses to sound, relative to rest, were often preserved or even amplified during propofol anesthesia, this does not imply that the brain continues to detect auditory novelty. To specifically evaluate the cortical responses to auditory novelty at two hierarchical levels, we probed the fMRI responses to local and global effects.

The local effect, contrasting local deviants to local standards, showed no significant activations during moderate propofol sedation, and this was replicated during deep propofol anesthesia. As a result, virtually all of the areas that were originally found responsive to local deviance in the awake monkey (Uhrig et al., 2014b) showed a stronger local effect in the awake state compared to propofol sedation. For both moderate and deep propofol anesthesia, these areas included the auditory cortex bilaterally, anterior cingulate gyrus (area 25), medial geniculate nucleus (auditory thalamus), striatum (left dorsal putamen, bilateral caudate), dorsal thalamus, medial superior temporal area and area V4 (Fig. 4a, b, d, e, g, h).

While these data indicate an essentially complete disruption of the local effect in propofol anesthesia, the response to global novelty, contrasting rare trials minus frequent trials, was partially preserved. During moderate propofol sedation, the global effect continued to activate the bilateral auditory cortex including core (A1, R), belt and parabelt regions, medial geniculate nucleus (auditory thalamus), the anterior cingulate cortex, prefrontal cortex areas 8 and 46, putamen and caudate (Fig. 5a, b). Virtually the same areas were replicated under deep propofol anesthesia (Fig. 5c, d). When comparing propofol sedation levels, there was even a stronger activation to the global effect under deep propofol anesthesia compared to moderate propofol sedation in the anterior cingulate cortex and caudate. Nevertheless, there was evidence that anesthesia did have a disruptive effect. We found no stronger activations during propofol anesthesia compared to the awake state, but conversely many areas showed a stronger global effect in the awake state than in moderate or deep propofol anesthesia. Those regions where propofol anesthesia decreased the response to global auditory novelty included the right prefrontal area 8A, bilateral premotor areas 6V, left parietal cortex (ventral intraparietal area, VIP), thalamus (parafascicular nucleus) and cerebellar dentate nuclei (Fig. 7a, b, d). They were jointly found in moderate and in deep sedation.

3.4. Local and Global novelties under deep ketamine anesthesia (Tables 2, 3)

During ketamine anesthesia, we again tested separately for local and global effects. The local effect continued to activate the parietal cortex (IPS), left superior temporal sulcus, putamen, V4, caudate and dorsal thalamus (Fig. 3a, b). Nevertheless, the local effect was significantly reduced during deep ketamine anesthesia compared to the awake state in the auditory cortex, medial geniculate nucleus (auditory thalamus), left dorsal putamen, medial superior temporal area and area V4 (Fig. 4c, f, i).

For the global effect, we found no significant activations under ketamine anesthesia. As a result, virtually all of the large set of regions that were previously shown to respond to global novelty in the awake state (Uhrig et al., 2014b) showed a significantly reduced global effect under ketamine anesthesia. Those included the anterior and posterior cingulate, prefrontal areas 8A, premotor areas 6V, left parietal cortex (VIP), striatum (bilateral putamen, left caudate), thalamus (parafascicular nucleus), auditory cortex A1, temporoparietal area TPt and cerebellar dentate nuclei (Fig. 6c, d). No differences were found in the other direction.

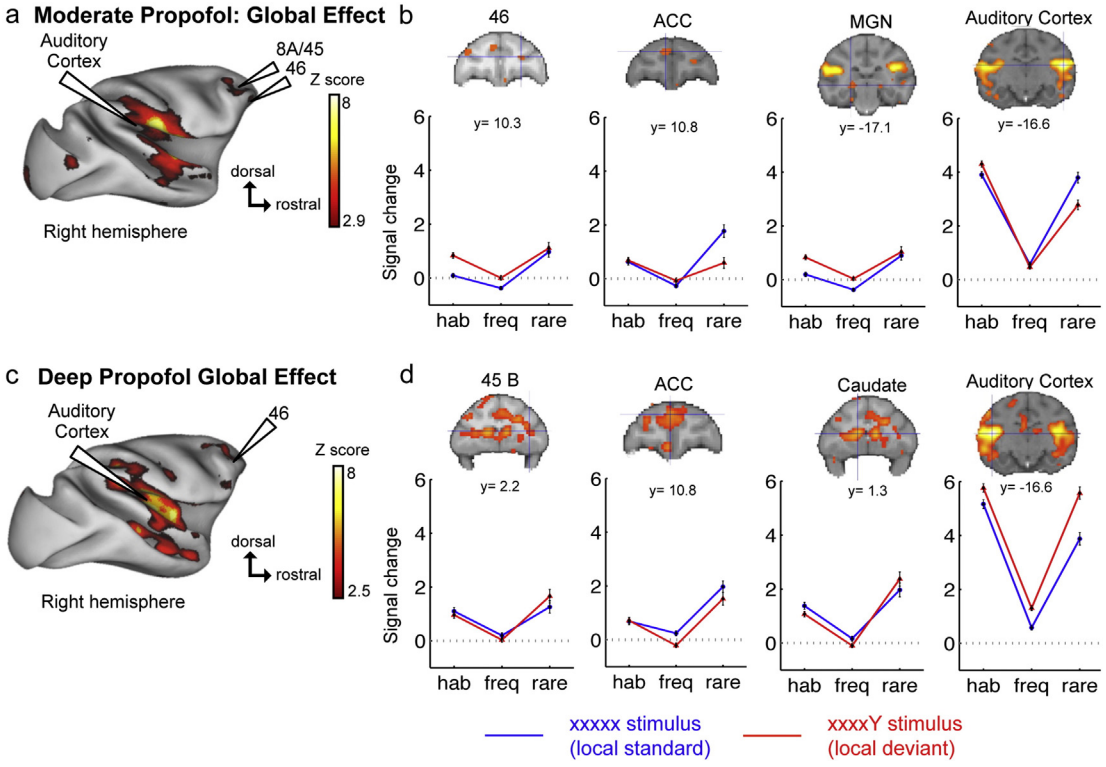

Fig. 5. Global novelty effect under anesthesia. a, Activation maps for the global novelty effect (rare minus frequent sequences = (xxxxx rare global deviants + xxxxY rare global deviants) − (xxxxx frequent global standards + xxxxY frequent global standards)) under moderate propofol sedation. b, fMRI signal change in areas responsive to the global effect (blue cross on SPM maps) under moderate propofol sedation. Plots show signal change for habituation (hab), frequent (freq) and rare stimuli. c, Activation maps for the global novelty effect under deep propofol anesthesia. d, fMRI signal change in areas responsive to global effect (blue cross on SPM maps) under deep propofol anesthesia. Plots show signal change for habituation (hab), frequent (freq) and rare stimuli. y, level of coronal section relative to the bregma in the Paxinos atlas. y, level of coronal section relative to the bregma in the Paxinos atlas. 46, prefrontal cortex area 46; 8A/45, prefrontal cortex area 8A/45; ACC, anterior cingulate cortex; MGN, medial geniculate nucleus. We found no significant activations for the global novelty effect under ketamine anesthesia. (For interpretation of the references to colour in this figure legend, the reader is referred to the web version of this article.)

3.5. Propagation of auditory violation signals across the monkey brain under propofol and ketamine anesthesia

To evaluate how auditory inputs propagate in the anesthetized brain, we used an event-related functional correlation analysis (PPI), which examines how the functional correlation of any brain area to the auditory cortex core region A1 is modulated by local or global effects. In agreement with the disappearance of the local effect during propofol anesthesia, the local effect did not induce any increase in functional correlation anywhere in the brain, neither during moderate nor during deep propofol anesthesia. During global deviants however (compared to global standards), moderate propofol sedation relative to the awake state induced a reduction in functional coupling between auditory cortex and the posterior cingulate cortex and the bilateral caudate (Supplementary Fig. 3a). When comparing deep propofol anesthesia with the awake state, functional correlation with A1 again decreased with anesthesia in the posterior cingulate cortex/precuneus, the bilateral caudate, and extended to additional regions in parietal cortex (VIP), dorsal bank of STS and visual areas V4/TEO (Supplementary Fig. 3b). Direct comparison of the two anesthesia levels further confirmed that functional correlation with area A1 decreased from moderate to deep propofol anesthesia for the global effect in the parietal cortex (VIP). In the converse direction, we found no increase in functional correlation during either moderate or deep propofol anesthesia compared to the awake state.

While these findings suggest that propofol anesthesia induces a partial functional disconnection of subcortical and cortical structures from auditory inputs, this disconnection was by no means complete. During anesthesia, several areas continued to show an increased functional connection with A1 for global deviants relative to global standard. Such an increase in functional correlation was found during moderate sedation in left prefrontal cortex (area 8, 46), premotor area 6V, left putamen, parietal cortex, medium superior temporal area, posterior cingulate cortex, visual areas V4 and anterior cingulate cortex (Fig. 8a); and during deep propofol anesthesia in bilateral prefrontal area 46, anterior cingulate cortex (areas 24, 32) and caudate (Fig. 8b).

During ketamine anesthesia, functional connectivity analysis revealed no increase in functional correlation with auditory cortex (A1) for the local effect or the global effect. Rather, we observed a strong reduction in functional connectivity relative to the awake state, for global deviants relative to global standards, in posterior cingulate cortex/precuneus, caudate, prefrontal cortex, area 8A, left parietal cortex (VIP), dorsal bank of STS and visual areas V4/TEO (Supplementary Fig. 3c).

3.6. Comparison between deep propofol and deep ketamine anesthesia

The results so far suggest some commonalities but also important differences in cortical activation under propofol and ketamine anesthesia. To formally evaluate these differences, we entered the deep propofol and deep ketamine data in a single SPM model. The results confirmed several of the above observations. First, pooling over all auditory stimuli relative to rest, we observed a stronger activation under propofol than under ketamine anesthesia in the auditory cortex including core (A1, R), belt and parabelt regions, anterior cingulate cortex, caudate and premotor area 6V. For global standard sequences, we found no differences between the deep propofol sedation and deep ketamine sedation, but for rare global deviant sequences relative to rest, a stronger activation during propofol sedation was again observed in the auditory cortex, anterior cingulate cortex, prefrontal cortex area 46, premotor area 6V, putamen and caudate. These results confirm that propofol, more than ketamine, leaves auditory cortex and anterior prefronto-subcortical areas in an activatable state, which may even exceed the awake state.

This conclusion was strengthened by the observation that while the local effect did not differ between deep propofol and deep ketamine

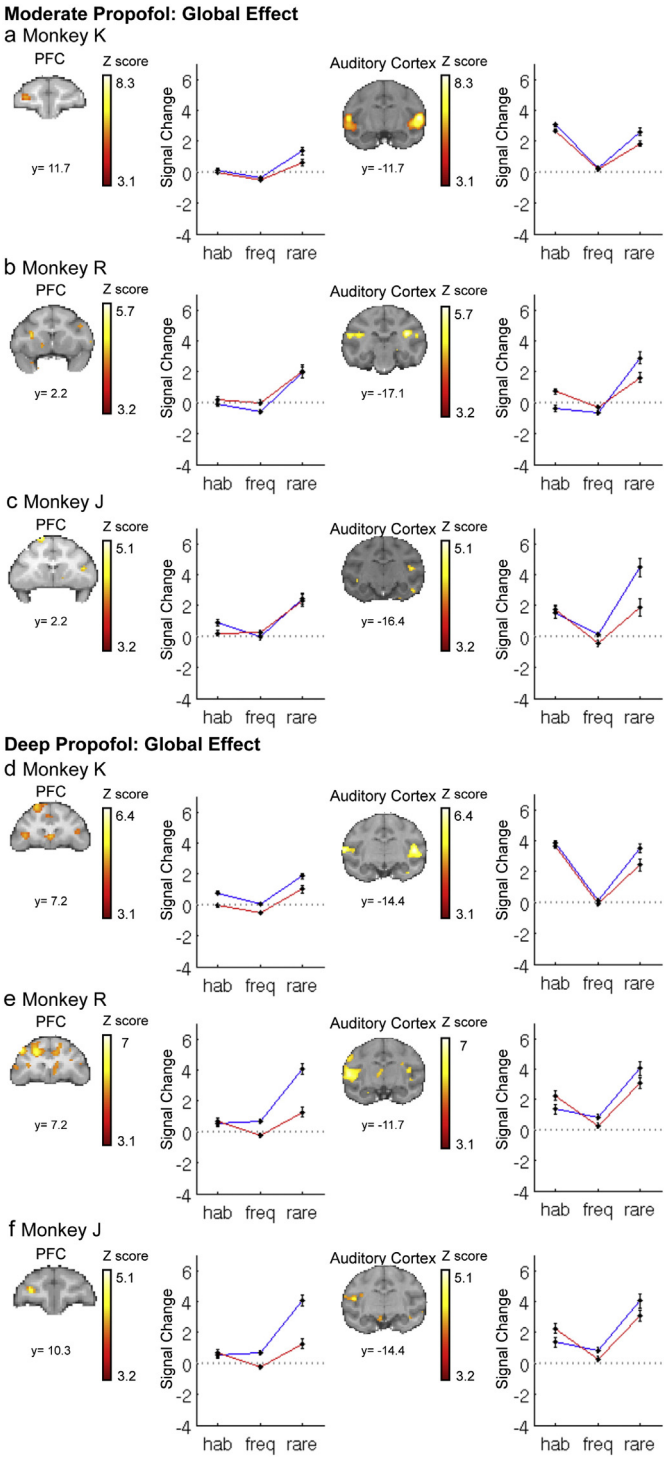

Fig. 6. Global novelty effect under anesthesia, individual results. Activation maps for rare minus frequent sequences (global novelty) under moderate and deep propofol anesthesia. fMRI signal change in areas responsive to global novelty. Plots show signal change for habituation (hab), frequent (freq) and rare stimuli. y, level of coronal section relative to the bregma in the Paxinos atlas. Individual results. $p < 0.001$ uncorrected Moderate propofol sedation. a, Monkey K: Activation map for the global effect in prefrontal cortex (PFC) and in the auditory cortex under moderate propofol sedation. b, Monkey R: Activation map for the global effect in prefrontal cortex (PFC) and in the auditory cortex under moderate propofol sedation. c, Monkey J: Activation map for the global effect in prefrontal cortex (PFC) and in the auditory cortex under moderate propofol sedation. Deep propofol anesthesia. d, Monkey K: Activation map for the global effect in prefrontal cortex (PFC) and in the auditory cortex under deep propofol anesthesia. e, Monkey R: Activation map for the global effect in prefrontal cortex (PFC) and in the auditory cortex under deep propofol anesthesia. f, Monkey J: Activation map for the global effect in prefrontal cortex (PFC) and in the auditory cortex under deep propofol anesthesia.

anesthesia, the global effect showed a stronger activation under propofol than under ketamine anesthesia in auditory cortex, anterior cingulate cortex (area 24), prefrontal areas 46 and 8A, premotor areas 6V, caudate and dorsal putamen (Supplementary Fig. 2). There was also a stronger increase in functional correlation with the auditory cortex during the global effect in the deep propofol anesthesia state compared to the deep ketamine anesthesia in the anterior cingulate cortex and prefrontal cortex area 46 (Supplementary Fig. 4, Supplementary Table 14).

4. Discussion

Our main finding is that both anesthetics, propofol and ketamine, while leaving intact or even enhancing the response to auditory cortical inputs, disrupt higher-order auditory novelty detection through a partial or total suppression of a fronto-parietal network.

4.1. Auditory processing under anesthesia

At all anesthesia levels, auditory stimuli still activated the auditory cortex, demonstrating a persistence of feed-forward cortical responses even at deep levels of anesthesia, in agreement with prior research (Ku et al., 2011; Lee et al., 2013). Primary sensory cortices remain receptive to incoming sensory information during anesthesia (Ypparila et al., 2002; Heinke et al., 2004a; Dueck et al., 2005; Koelsch et al., 2006; Adapa et al., 2014), supporting the idea that conscious perceptual experience does not correlate with the neuronal activity in primary sensory areas (Crick and Koch, 2003).

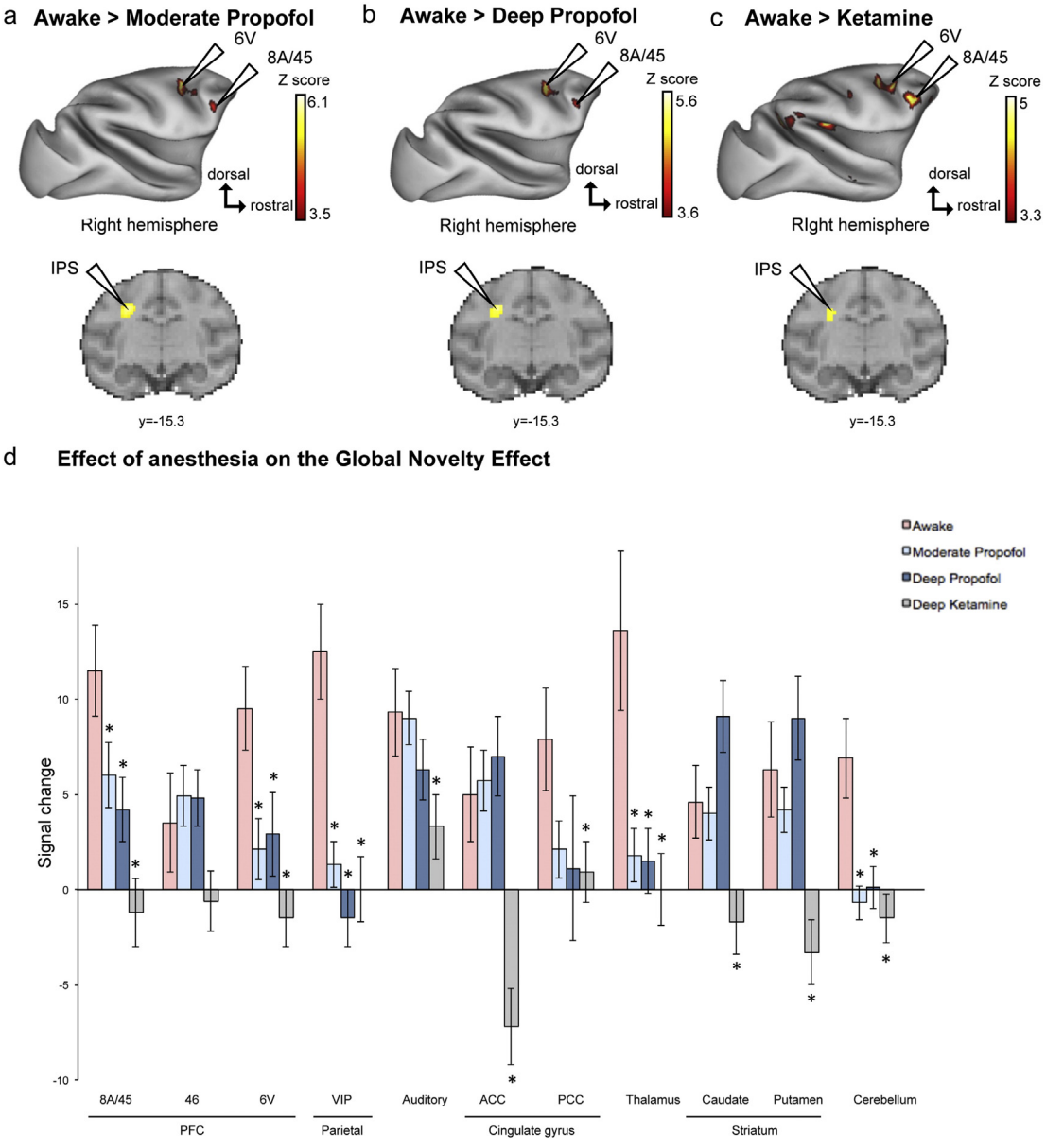

Fig. 7. Comparison between the awake state and anesthesia states for the global novelty effect. a, Activation map for the global novelty effect showing stronger activations in the awake state compared to moderate propofol sedation; b, Activation map for the global novelty effect with stronger activations in the awake state compared to deep propofol anesthesia; c, Activation map for the global novelty effect showing stronger activations in the awake state then under deep ketamine anesthesia. Group analysis, $p < 0.05$, FDR corrected. d, fMRI signal change in areas responsive to the global novelty effect for the awake state (red), moderate propofol sedation (light blue); deep propofol anesthesia (dark blue) and deep ketamine anesthesia (grey). * significant changes to global novelty between the awake state and the anesthesia states (moderate propofol sedation, deep propofol anesthesia, deep ketamine anesthesia). 8A/45, prefrontal cortex area 8A/45; 6V, premotor area 6V; IPS, intraparietal sulcus; PFC, prefrontal cortex; VIP, ventral intraparietal area; ACC, anterior cingulate cortex; PCC, posterior cingulate cortex. (For interpretation of the references to colour in this figure legend, the reader is referred to the web version of this article.)

Remarkably, auditory activation relative to rest was stronger under anesthesia than in the awake state. This novel finding may be tentatively attributed to a lack of top-down executive control of attention and feedback under anesthesia (Hudetz, 2009; Mashour, 2014). During the awake state, a powerful control is exerted by anterior areas over the posterior regions of the brain, either selectively amplifying relevant inputs or, on the contrary, repressing irrelevant or predictable ones. General anesthesia reduces such fronto-parietal feedback connectivity (Hudetz, 2009; Lee et al., 2009a; Lee et al., 2013) while preserving feedforward connectivity (Lee et al., 2009a; Ku et al., 2011; Lee et al., 2013). The net result may therefore be a stronger automatic and bottom-up propagation of external stimuli to anterior cortical regions, as observed here.

For global deviants, auditory activity propagated beyond primary auditory cortex, even including dorsolateral prefrontal cortex, anterior cingulate cortex and basal ganglia, but with a specific disruption of functional connectivity to parietal cortex. A previous study showed that light anesthesia preserves auditory processing of words beyond the auditory cortex, in the frontal, parietal and occipital cortices (Kerssens et al., 2005). Although auditory processing of complex stimuli is affected even by light anesthesia (Heinke et al., 2004a; Plourde et al., 2006; Davis et al., 2007; Liu et al., 2012; Adapa et al., 2014), the presentation of auditory sentences may still activate multiple areas of temporal cortex under sedation (Davis et al., 2007), suggesting that basic speech processing can be preserved under sedation. However, activation corresponding to a higher level of language processing (indexing syntactic and semantic processes by comparing ambiguous versus non-ambiguous sentences), vanishes from inferior frontal and posterior temporal regions during sedation (Davis et al., 2007), suggesting that anesthetics abolish higher-level speech processing. Anesthesia, not only affects higher auditory stimuli processing, but also visual stimuli processing in higher-order association cortices, such as the parietal cortex and the insula, whereas visual processing is preserved in subcortical structures and primary visual cortex under anesthesia (Martin et al., 2000, Heinke and Schwarzbauer, 2001; Ramani et al., 2007).

Using an auditory paradigm with two well-defined hierarchical levels of auditory complexity, the local-global paradigm, we found fMRI activations that are consistent with the literature, i.e. showing that anesthesia impairs cortical sensory processing for stimuli with higher complexity (MacDonald et al., 2015). However, this disruption was only partial. We first discuss the activations that were jointly disrupted by both anesthetics, then the paradoxical preservation of novelty effects in some conditions.

4.2. Role of the parietal cortex and the thalamus

In our data, all anesthetics and all levels of anesthesia disrupted parietal cortex and thalamic nuclei activity. The extent of parietal cortex disorganization also reflected the depth of anesthesia: although both propofol doses suppressed the parietal response to the global effect, moderate propofol sedation showed a persistent functional correlation between A1 and VIP in the event-related PPI analysis. A previous study showed that word stimuli under light anesthesia may still activate the parietal cortex (Kerssens et al., 2005), but most previous studies suggest that parietal areas are most strongly affected by anesthetics (Kaisti et al., 2002; Alkire et al., 2008), with a relative preservation of early fronto-parietal feed-forward connections (Imas et al., 2005; Lee et al., 2009a). Fronto-parietal feedback is abolished by propofol (Lee et al., 2009b; Boly et al., 2012; Lee et al., 2013), which may explain our finding that, during propofol anesthesia, information about novel sounds is still present in the prefrontal cortex (presumably propagated

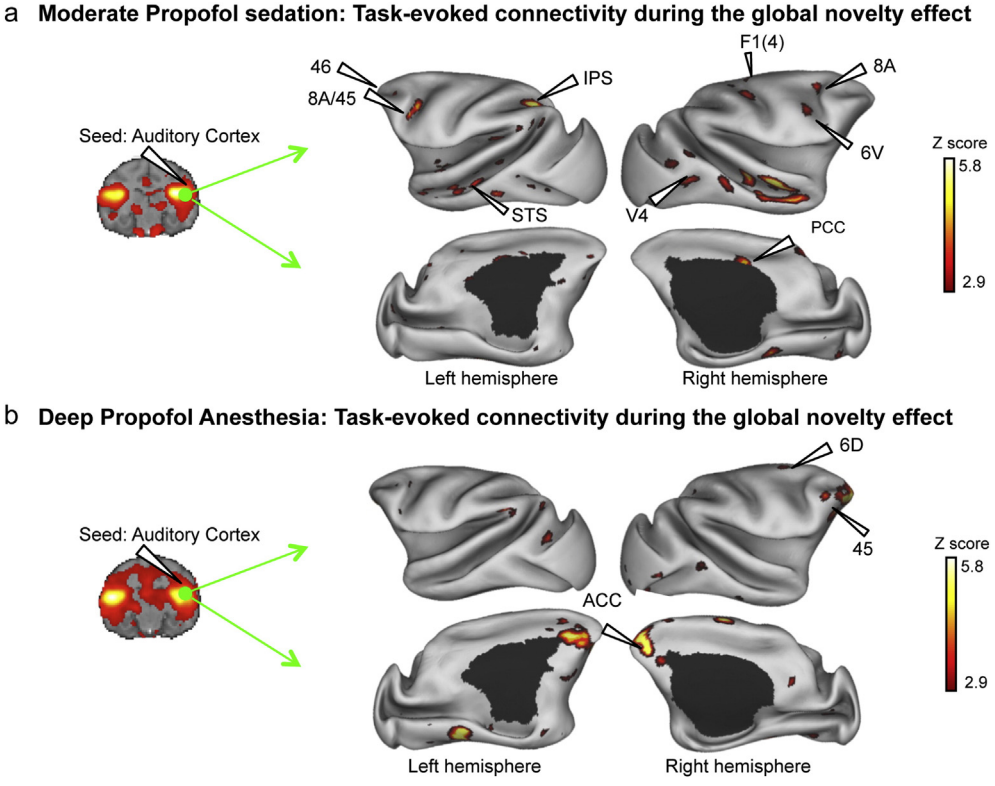

Fig. 8. Task-evoked connectivity during the global novelty effect. a, Task-evoked connectivity during the global novelty effect in the macaque cortex under moderate propofol sedation, using a seed in the right auditory cortex and looking for psychophysiological interaction, i.e. increase in correlation with auditory cortex activation in response to rare than to frequent sequences. b, Task-evoked connectivity during the global novelty effect in the macaque cortex under deep propofol anesthesia, using a seed in the right auditory cortex and looking for psychophysiological interaction. Group analysis, $p < 0.05$, FDR corrected. 8A/45, prefrontal cortex area 8A/45; 46, prefrontal cortex area 46; 6V, premotor area 6V; ACC, anterior cingulate cortex; IPS, intraparietal sulcus; STS, superior temporal sulcus, PCC, posterior cingulate cortex, V4, visual areas V4. Functional connectivity analysis revealed no increase in functional correlation with auditory cortex (A1) during ketamine anesthesia.

there via preserved feed-forward connections), but not transmitted to the parietal cortex.

At the subcortical level, thalamic activity was profoundly affected by anesthesia (Alkire et al., 2000; Schiff and Plum, 2000; Franks, 2008). It should be noted that distinct thalamic nuclei were affected by local and global effects: anesthesia disrupted local novelty response in the auditory thalamus (MGN) and global novelty detection in the intralaminar thalamic nuclei (parafascicular nucleus).

4.3. Does predictive coding continue to operate under anesthesia?

We used the local/global test to dissociate two hierarchical levels of auditory novelty processing (Bekinschtein et al., 2009; Wacongne et al., 2012; Strauss et al., 2015).

We found stronger activations to local violations in the auditory cortex of awake macaques as previously reported (Gil-da-Costa et al., 2013; Uhrig et al., 2014b), reflecting the MMN in previous studies (Czigler et al., 2007; Bekinschtein et al., 2009; Wacongne et al., 2012). This "mismatch response" is thought to involve, at least in part (Strauss et al., 2015), a violation of an expectation generated on the basis of initial tone repetition (xxxx, followed by Y). The generation of these expectations is thought to require short-term plasticity of glutamatergic connections, either locally within the cortex (Wacongne et al., 2012) or in long-distance projections from prefrontal cortex (Garrido et al., 2008; Garrido et al., 2009). It should therefore not be surprising that this auditory activity strongly decrease or vanish with anesthetics that affect these cortical circuits either directly (Ketamine acting on NMDA receptors) or indirectly (propofol acting on GABA receptors).

Propofol anesthesia strongly affected the local effect, which persisted only under moderate propofol sedation and only if we lowered the statistical threshold to cluster ($p < 0.05$ without FDR correction). This is compatible with previous findings that the MN is abolished in humans during propofol-induced unconsciousness (Heinke et al., 2004b). Heinke et al. (2004b) also showed that the P3a, dependent on neuronal sources in frontal cortex (Näätanen, 2002), remained present during wakefulness and light propofol sedation, but disappeared during deep propofol sedation. As for ketamine, it also abolished fMRI responses to local violations in the auditory cortex with our anesthetic dose. Similarly, but at sub-anesthetic doses, ketamine was previously observed to reduce the amplitude of MMN (Umbricht et al., 2000; Kreitschmann-Andermahr et al., 2001; Heekeren et al., 2008; Schmidt et al., 2012; Schmidt et al., 2013). Other NMDA antagonists also abolish the MMN in the primary auditory cortex in monkeys (Javitt et al., 1996). The local effect is also reduced during the loss of consciousness associated with sleep (Strauss et al., 2015) or coma and vegetative state (Faugeras et al., 2012). Although the local effect does not fully vanish in those states, the component of the effect that remains may be related to sensory adaptation rather than to expectation violation (Strauss et al., 2015).

More surprisingly, we found that the local effect remained detectable under ketamine outside the auditory cortex, including intraparietal cortex, striatum and thalamus. Pending a replication, we can only speculate that these regions continue to receive sufficient bottom-up inputs from the auditory cortex to be activated and perhaps to adapt to the repeated sound. In future studies, more light could be shed on this point by separating sensory adaptation from predictive coding, for instance using an alternation paradigm (Wacongne et al., 2011; Todorovic and de Lange, 2012; Strauss et al., 2015).

The complete suppression of the global effect under ketamine anesthesia is comparable to observations during sleep (Strauss et al., 2015) or in patients with disorders of consciousness (Bekinschtein et al., 2009; Faugeras et al., 2012). It fits with the hypothesis that anesthesia, by preventing long-distance top-down cortico-cortical exchanges, strongly disrupts the ability of the brain to generate high-level predictive-coding signals (Imas et al., 2005; Lee et al., 2009a; Lee et al., 2013). However, an unexpected finding was that, under propofol anesthesia, even at a deep level, the processing of global deviant events continued to be observed within the auditory cortex and even in prefrontal areas 45 and 46. Particularly striking is the fact that, under propofol, the local effect vanished from the auditory cortex, only to be replaced by a global effect (Fig. 5b, d). This observation suggests a possible, though admittedly speculative interpretation, according to which propofol may have led to a temporal slowing and even possibly a fusion of the auditory responses to the five successive sounds in each trial, thus turning the global effect into a local effect. Indeed, if temporal separation was lost, the xxxxx and xxxxY sequences would merely be represented as two distinct "chords". As a result, there would be no temporal violation to the final sound in xxxxY, hence no local effect, but there could be adaptation of auditory responses to the frequent "chord" and recovery in response to the rare "chord", thus yielding a global effect. While fMRI does not have the temporal resolution needed to test this idea, further studies could use event-related potentials (Gil-da-Costa et al., 2013), MEG (Wacongne, Labyt et al., Strauss et al., 2015) or intracranial recordings (El Karoui et al., 2014) to track the fate of individual sounds under deep propofol anesthesia.

4.4. The global neuronal workspace under anesthesia

In awake macaques, second-order sequence violations activate a network comprising higher-order prefrontal, cingulate and parietal regions (Uhrig et al., 2014b), similar to the network activated in conscious humans (Bekinschtein et al., 2009). This network, putatively operating as a "global neuronal workspace" (Dehaene et al., 1998; Dehaene and Naccache, 2001; Baars, 2005; Shanahan and Baars, 2005; Dehaene and Changeux, 2011), has a potential anatomical substrate in the massive long-distance interconnections established in part by layer 2/3 pyramidal neurons (Goldman-Rakic, 1988). Ketamine completely suppressed the "global workspace" activation, probably due to its anti-NMDA direct action on glutamatergic synapses that may underlie long-distance GNW communication and operate primarily in a top-down manner (Dehaene et al., 1998; Self et al., 2012). Deep propofol anesthesia disrupted the "global workspace" responses only partially, preserving prefrontal and anterior cingulate responses.

According to the GNW model, conscious processing requires a global long-distance broadcasting of information to interconnected prefrontal, cingulate and parietal areas (Dehaene et al., 2006; Gaillard et al., 2009). Although propofol directly affects brainstem and thalamic nuclei, unconsciousness induced by propofol may result from a partial breakdown of information integration at the cortical level (John, 2001; Mashour, 2004; Ferrarelli et al., 2010). Propofol sedation has been reported to result in a strong disruption of the interaction between low-order sensory cortices and higher-order fronto-parietal cortices (Boveroux et al., 2010), which is essential for the perception of external stimuli, with an impaired cortical top-down processing (Jordan et al., 2013).

5. Conclusion

Our most important conclusion is that two different categories of anesthetics, which act at different receptors and different neuronal sites, have the convergent effect of disrupting, either totally (ketamine) or partially (propofol), a prefrontal-parietal network, suggesting that anesthesia reduces higher-order cortical activations. Although it is difficult to test awareness in monkeys, our findings are in line with the growing evidence that the coordinated activation of this fronto-parietal network, particularly in its posterior nodes in parietal cortex and precuneus, is necessary for conscious processing of information (Alkire et al., 2008; Ferrarelli et al., 2010; Dehaene and Changeux, 2011). It is consistent with the hypothesis that a disruption of long-distance cortico-cortical and cortico-thalamic networks may be one mechanism through which anesthetics induce loss of consciousness (Velly et al., 2007; Monti et al., 2013).

Conflict of interest

The authors declare no competing financial interests.

Acknowledgments

This work was supported by the European Research Council (ERC grant 249830 NeuroConsc to S.D.), Inserm Avenir program to B.J., Collège de France, CEA Neurospin and Bettencourt-Schueller Foundation. We thank Morgan Dupont and Wilfried Pianezzola for help with behavioral and anesthesia experiments, Alexis Amadon, Hauke Kolster, Laurent Laribière and the NeuroSpin MRI and informatics teams for help with imaging tools, Christophe Joubert, and Jean-Marie Helies for animal facilities, and Michel Bottlaender, Jean-Robert Deverre and Denis Le Bihan for support. This work was performed on a platform of France Life Imaging network partly funded by the grant "ANR-11-INBS-0006".

Appendix A. Supplementary data

Supplementary data to this article can be found online at http://dx.doi.org/10.1016/j.neuroimage.2016.08.004.

References

Absalom, A., Kenny, G., 2005. Paedfusor' pharmacokinetic data set. Br. J. Anaesth. 95 (1), 110.

Adapa, R.M., Davis, M.H., Stamatakis, E.A., Absalom, A.R., Menon, D.K., 2014. Neural correlates of successful semantic processing during propofol sedation. Hum. Brain Mapp. 35 (7), 2935–2949.

Alkire, M.T., Haier, R.J., Fallon, J.H., 2000. Toward a unified theory of narcosis: brain imaging evidence for a thalamocortical switch as the neurophysiologic basis of anesthetic-induced unconsciousness. Conscious. Cogn. 9 (3), 370–386.

Alkire, M.T., Hudetz, A.G., Tononi, G., 2008. Consciousness and anesthesia. Science 322 (5903), 876–880.

Baars, B.J., 2005. Global workspace theory of consciousness: toward a cognitive neuroscience of human experience. Prog. Brain Res. 150, 45–53.

Barttfeld, P., Uhrig, L., Sitt, J.D., Sigman, M., Jarraya, B., Dehaene, S., 2015. Signature of consciousness in the dynamics of resting-state brain activity. Proc. Natl. Acad. Sci. U. S. A. 112 (3), 887–892.

Bekinschtein, T.A., Dehaene, S., Rohaut, B., Tadel, F., Cohen, L., Naccache, L., 2009. Neural signature of the conscious processing of auditory regularities. Proc. Natl. Acad. Sci. U. S. A. 106 (5), 1672–1677.

Boly, M., Moran, R., Murphy, M., Boveroux, P., Bruno, M.A., Noirhomme, Q., Ledoux, D., Bonhomme, V., Brichant, J.F., Tononi, G., Laureys, S., Friston, K., 2012. Connectivity changes underlying spectral EEG changes during propofol-induced loss of consciousness. J. Neurosci. 32 (20), 7082–7090.

Boveroux, P., Vanhaudenhuyse, A., Bruno, M.A., Noirhomme, Q., Lauwick, S., Luxen, A., Degueldre, C., Plenevaux, A., Schnakers, C., Phillips, C., Brichant, J.F., Bonhomme, V., Maquet, P., Greicius, M.D., Laureys, S., Boly, M., 2010. Breakdown of within- and between-network resting state functional magnetic resonance imaging connectivity during propofol-induced loss of consciousness. Anesthesiology 113 (5), 1038–1053.

Brown, E.N., Lydic, R., Schiff, N.D., 2010. General anesthesia, sleep, and coma. N. Engl. J. Med. 363 (27), 2638–2650.

Buckner, R.L., Andrews-Hanna, J.R., Schacter, D.L., 2008. The brain's default network: anatomy, function, and relevance to disease. Ann. N. Y. Acad. Sci. 1124, 1–38.

Ching, S., Cimenser, A., Purdon, P.L., Brown, E.N., Kopell, N.J., 2010. Thalamocortical model for a propofol-induced alpha-rhythm associated with loss of consciousness. Proc. Natl. Acad. Sci. U. S. A. 107 (52), 22665–22670.

Cimenser, A., Purdon, P.L., Pierce, E.T., Walsh, J.L., Salazar-Gomez, A.F., Harrell, P.G., Tavares-Stoeckel, C., Habeeb, K., Brown, E.N., 2011. Tracking brain states under general anesthesia by using global coherence analysis. Proc. Natl. Acad. Sci. U. S. A. 108 (21), 8832–8837.

Crick, F., Koch, C., 2003. A framework for consciousness. Nat. Neurosci. 6 (2), 119–126.

Czigler, I., Weisz, J., Winkler, I., 2007. Backward masking and visual mismatch negativity: electrophysiological evidence for memory-based detection of deviant stimuli. Psychophysiology 44 (4), 610–619.

Davis, M.H., Coleman, M.R., Absalom, A.R., Rodd, J.M., Johnsrude, I.S., Matta, B.F., Owen, A.M., Menon, D.K., 2007. Dissociating speech perception and comprehension at reduced levels of awareness. Proc. Natl. Acad. Sci. U. S. A. 104 (41), 16032–16037.

Dehaene, S., Changeux, J.P., 2011. Experimental and theoretical approaches to conscious processing. Neuron 70 (2), 200–227.

Dehaene, S., Naccache, L., 2001. Towards a cognitive neuroscience of consciousness: basic evidence and a workspace framework. Cognition 79 (1–2), 1–37.

Dehaene, S., Kerszberg, M., Changeux, J.P., 1998. A neuronal model of a global workspace in effortful cognitive tasks. Proc. Natl. Acad. Sci. U. S. A. 95 (24), 14529–14534.

Dehaene, S., Changeux, J.P., Naccache, L., Sackur, J., Sergent, C., 2006. Conscious, preconscious, and subliminal processing: a testable taxonomy. Trends Cogn. Sci. 10 (5), 204–211.

Dueck, M.H., Petzke, F., Gerbershagen, H.J., Paul, M., Hesselmann, V., Girnus, R., Krug, B., Sorger, B., Goebel, R., Lehrke, R., Sturm, V., Boerner, U., 2005. Propofol attenuates responses of the auditory cortex to acoustic stimulation in a dose-dependent manner: a FMRI study. Acta Anaesthesiol. Scand. 49 (6), 784–791.

El Karoui, I., King, J.R., Sitt, J., Meyniel, F., Van Gaal, S., Hasboun, D., Adam, C., Navarro, V., Baulac, M., Dehaene, S., Cohen, L., Naccache, L., 2014. Event-related potential, time-frequency, and functional connectivity facets of local and global auditory novelty processing: an intracranial study in humans. Cereb, Cortex.

Faugeras, F., Rohaut, B., Weiss, N., Bekinschtein, T.A., Galanaud, D., Puybasset, L., Bolgert, F., Sergent, C., Cohen, L., Dehaene, S., Naccache, L., 2011. Probing consciousness with event-related potentials in the vegetative state. Neurology 77 (3), 264–268.

Faugeras, F., Rohaut, B., Weiss, N., Bekinschtein, T., Galanaud, D., Puybasset, L., Bolgert, F., Sergent, C., Cohen, L., Dehaene, S., Naccache, L., 2012. Event related potentials elicited by violations of auditory regularities in patients with impaired consciousness. Neuropsychologia 50 (3), 403–418.

Ferrarelli, F., Massimini, M., Sarasso, S., Casali, A., Riedner, B.A., Angelini, G., Tononi, G., Pearce, R.A., 2010. Breakdown in cortical effective connectivity during midazolam-induced loss of consciousness. Proc. Natl. Acad. Sci. U. S. A. 107 (6), 2681–2686.

Feshchenko, V.A., Veselis, R.A., Reinsel, R.A., 2004. Propofol-induced alpha rhythm. Neuropsychobiology 50 (3), 257–266.

Franks, N.P., 2008. General anaesthesia: from molecular targets to neuronal pathways of sleep and arousal. Nat. Rev. Neurosci. 9 (5), 370–386.

Frey, S., Pandya, D.N., Chakravarty, M.M., Bailey, L., Petrides, M., Collins, D.L., 2011. An MRI based average macaque monkey stereotaxic atlas and space (MNI monkey space). NeuroImage 55 (4), 1435–1442.

Friston, K.J., Buechel, C., Fink, G.R., Morris, J., Rolls, E., Dolan, R.J., 1997. Psychophysiological and modulatory interactions in neuroimaging. NeuroImage 6 (3), 218–229.

Gaillard, R., Dehaene, S., Adam, C., Clemenceau, S., Hasboun, D., Baulac, M., Cohen, L., Naccache, L., 2009. Converging intracranial markers of conscious access. PLoS Biol. 7 (3), e61.

Garrido, M.I., Friston, K.J., Kiebel, S.J., Stephan, K.E., Baldeweg, T., Kilner, J.M., 2008. The functional anatomy of the MMN: a DCM study of the roving paradigm. NeuroImage 42 (2), 936–944.

Garrido, M.I., Kilner, J.M., Kiebel, S.J., Friston, K.J., 2009. Dynamic causal modeling of the response to frequency deviants. J. Neurophysiol. 101 (5), 2620–2631.

Gil-da-Costa, R., Stoner, G.R., Fung, R., Albright, T.D., 2013. Nonhuman primate model of schizophrenia using a noninvasive EEG method. Proc. Natl. Acad. Sci. U. S. A. 110 (38), 15425–15430.

Goldman-Rakic, P.S., 1988. Topography of cognition: parallel distributed networks in primate association cortex. Annu. Rev. Neurosci. 11, 137–156.

Heekeren, K., Daumann, J., Neukirch, A., Stock, C., Kawohl, W., Norra, C., Waberski, T.D., Gouzoulis-Mayfrank, E., 2008. Mismatch negativity generation in the human 5HT2A agonist and NMDA antagonist model of psychosis. Psychopharmacology 199 (1), 77–88.

Heinke, W., Schwarzbauer, C., 2001. Subanesthetic isoflurane affects task-induced brain activation in a highly specific manner: a functional magnetic resonance imaging study. Anesthesiology 94 (6), 973–981.

Heinke, W., Fiebach, C.J., Schwarzbauer, C., Meyer, M., Olthoff, D., Alter, K., 2004a. Sequential effects of propofol on functional brain activation induced by auditory language processing: an event-related functional magnetic resonance imaging study. Br. J. Anaesth. 92 (5), 641–650.

Heinke, W., Kenntner, R., Gunter, T.C., Sammler, D., Olthoff, D., Koelsch, S., 2004b. Sequential effects of increasing propofol sedation on frontal and temporal cortices as indexed by auditory event-related potentials. Anesthesiology 100 (3), 617–625.

Hudetz, A.G., 2009. Feedback suppression in anesthesia. Is it reversible? Conscious. Cogn. 18 (4), 1079–1081.

Hudetz, A.G., Vizuete, J.A., Imas, O.A., 2009. Desflurane selectively suppresses long-latency cortical neuronal response to flash in the rat. Anesthesiology 111 (2), 231–239.

Imas, O.A., Ropella, K.M., Ward, B.D., Wood, J.D., Hudetz, A.G., 2005. Volatile anesthetics disrupt frontal-posterior recurrent information transfer at gamma frequencies in rat. Neurosci. Lett. 387 (3), 145–150.

Javitt, D.C., Steinschneider, M., Schroeder, C.E., Arezzo, J.C., 1996. Role of cortical N-methyl-d-aspartate receptors in auditory sensory memory and mismatch negativity generation: implications for schizophrenia. Proc. Natl. Acad. Sci. U. S. A. 93 (21), 11962–11967.

John, E.R., 2001. A field theory of consciousness. Conscious. Cogn. 10 (2), 184–213.

Jordan, D., Ilg, R., Riedl, V., Schorer, A., Grimberg, S., Neufang, S., Omerovic, A., Berger, S., Untergehrer, G., Preibisch, C., Schulz, E., Schuster, T., Schroter, M., Spoormaker, V., Zimmer, C., Hemmer, B., Wohlschlager, A., Kochs, E.F., Schneider, G., 2013. Simultaneous electroencephalographic and functional magnetic resonance imaging indicate impaired cortical top-down processing in association with anesthetic-induced unconsciousness. Anesthesiology 119 (5), 1031–1042.

Kaisti, K.K., Metsahonkala, L., Teras, M., Oikonen, V., Aalto, S., Jaaskelainen, S., Hinkka, S., Scheinin, H., 2002. Effects of surgical levels of propofol and sevoflurane anesthesia on cerebral blood flow in healthy subjects studied with positron emission tomography. Anesthesiology 96 (6), 1358–1370.

Kerssens, C., Hamann, S., Peltier, S., Hu, X.P., Byas-Smith, M.G., Sebel, P.S., 2005. Attenuated brain response to auditory word stimulation with sevoflurane: a functional magnetic resonance imaging study in humans. Anesthesiology 103 (1), 11–19.

Koelsch, S., Heinke, W., Sammler, D., Olthoff, D., 2006. Auditory processing during deep propofol sedation and recovery from unconsciousness. Clin. Neurophysiol. 117 (8), 1746–1759.

Kreitschmann-Andermahr, I., Rosburg, T., Demme, U., Gaser, E., Nowak, H., Sauer, H., 2001. Effect of ketamine on the neuromagnetic mismatch field in healthy humans. Brain Res. Cogn. Brain Res. 12 (1), 109–116.

Ku, S.W., Lee, U., Noh, G.J., Jun, I.G., Mashour, G.A., 2011. Preferential inhibition of frontal-to-parietal feedback connectivity is a neurophysiologic correlate of general anesthesia in surgical patients. PLoS One 6 (10), e25155.
Lee, U., Kim, S., Noh, G.J., Choi, B.M., Hwang, E., Mashour, G.A., 2009a. The directionality and functional organization of frontoparietal connectivity during consciousness and anesthesia in humans. Conscious. Cogn. 18 (4), 1069–1078.
Lee, U., Mashour, G.A., Kim, S., Noh, G.J., Choi, B.M., 2009b. Propofol induction reduces the capacity for neural information integration: implications for the mechanism of consciousness and general anesthesia. Conscious. Cogn. 18 (1), 56–64.
Lee, U., Ku, S., Noh, G., Baek, S., Choi, B., Mashour, G.A., 2013. Disruption of frontal-parietal communication by ketamine, propofol, and sevoflurane. Anesthesiology 118 (6), 1264–1275.
Liu, X., Lauer, K.K., Ward, B.D., Rao, S.M., Li, S.J., Hudetz, A.G., 2012. Propofol disrupts functional interactions between sensory and high-order processing of auditory verbal memory. Hum. Brain Mapp. 33 (10), 2487–2498.
MacDonald, A.A., Naci, L., MacDonald, P.A., Owen, A.M., 2015. Anesthesia and neuroimaging: investigating the neural correlates of unconsciousness. Trends Cogn. Sci. 19 (2), 100–107.
Mantini, D., Gerits, A., Nelissen, K., Durand, J.B., Joly, O., Simone, L., Sawamura, H., Wardak, C., Orban, G.A., Buckner, R.L., Vanduffel, W., 2011. Default mode of brain function in monkeys. J. Neurosci. 31 (36), 12954–12962.
Martin, E., Thiel, T., Joeri, P., Loenneker, T., Ekatodramis, D., Huisman, T., Hennig, J., Marcar, V.L., 2000. Effect of pentobarbital on visual processing in man. Hum. Brain Mapp. 10 (3), 132–139.
Mashour, G.A., 2004. Consciousness unbound: toward a paradigm of general anesthesia. Anesthesiology 100 (2), 428–433.
Mashour, G.A., 2014. Top-down mechanisms of anesthetic-induced unconsciousness. Front. Syst. Neurosci. 8, 115.
Monti, M.M., L., E.S., Rubinov, M., Boveroux, P., Vanhaudenhuyse, A., Gosseries, O., Bruno, M.A., Noirhomme, Q., Boly, M., Laureys, S., 2013. Dynamic change of global and local information processing in propofol-induced loss and recovery of consciousness. PLoS Comput. Biol. 9, e1003271.
Murphy, M., Bruno, M.A., Riedner, B.A., Boveroux, P., Noirhomme, Q., Landsness, E.C., Brichant, J.F., Phillips, C., Massimini, M., Laureys, S., Tononi, G., Boly, M., 2011. Propofol anesthesia and sleep: a high-density EEG study. Sleep 34 (3), 283–291A.
Näätanen, R.A.K., 2002. Electrophysiology of Attention in Stevens Handbook of Experimental Psycholoy. John Wiley, New York.
Oizumi, M., Albantakis, L., Tononi, G., 2014. From the phenomenology to the mechanisms of consciousness: integrated information theory 3.0. PLoS Comput. Biol. 10 (5), e1003588.
Pinault, D., 2008. N-methyl d-aspartate receptor antagonists ketamine and MK-801 induce wake-related aberrant gamma oscillations in the rat neocortex. Biol. Psychiatry 63 (8), 730–735.
Plourde, G., Belin, P., Chartrand, D., Fiset, P., Backman, S.B., Xie, G., Zatorre, R.J., 2006. Cortical processing of complex auditory stimuli during alterations of consciousness with the general anesthetic propofol. Anesthesiology 104 (3), 448–457.
Purdon, P.L., Pierce, E.T., Mukamel, E.A., Prerau, M.J., Walsh, J.L., Wong, K.F., Salazar-Gomez, A.F., Harrell, P.G., Sampson, A.L., Cimenser, A., Ching, S., Kopell, N.J., Tavares-Stoeckel, C., Habeeb, K., Merhar, R., Brown, E.N., 2013. Electroencephalogram signatures of loss and recovery of consciousness from propofol. Proc. Natl. Acad. Sci. U. S. A. 110 (12), E1142–E1151.
Purdon, P.L., Sampson, A., Pavone, K.J., Brown, E.N., 2015. Clinical electroencephalography for anesthesiologists: part I: background and basic signatures. Anesthesiology 123 (4), 937–960.
Ramani, R., Qiu, M., Constable, R.T., 2007. Sevoflurane 0.25 MAC preferentially affects higher order association areas: a functional magnetic resonance imaging study in volunteers. Anesth. Analg. 105 (3), 648–655.
Schiff, N.D., Plum, F., 2000. The role of arousal and "gating" systems in the neurology of impaired consciousness. J. Clin. Neurophysiol. 17 (5), 438–452.
Schmidt, A., Bachmann, R., Kometer, M., Csomor, P.A., Stephan, K.E., Seifritz, E., Vollenweider, F.X., 2012. Mismatch negativity encoding of prediction errors predicts S-ketamine-induced cognitive impairments. Neuropsychopharmacology 37 (4), 865–875.
Schmidt, A., Diaconescu, A.O., Kometer, M., Friston, K.J., Stephan, K.E., Vollenweider, F.X., 2013. Modeling ketamine effects on synaptic plasticity during the mismatch negativity. Cereb. Cortex 23 (10), 2394–2406.
Schuttler, J., Stanski, D.R., White, P.F., Trevor, A.J., Horai, Y., Verotta, D., Sheiner, L.B., 1987. Pharmacodynamic modeling of the EEG effects of ketamine and its enantiomers in man. J. Pharmacokinet. Biopharm. 15 (3), 241–253.
Self, M.W., Kooijmans, R.N., Super, H., Lamme, V.A., Roelfsema, P.R., 2012. Different glutamate receptors convey feedforward and recurrent processing in macaque V1. Proc. Natl. Acad. Sci. U. S. A. 109 (27), 11031–11036.
Shanahan, M., Baars, B., 2005. Applying global workspace theory to the frame problem. Cognition 98 (2), 157–176.
Steriade, M., Nunez, A., Amzica, F., 1993. A novel slow (<1 Hz) oscillation of neocortical neurons in vivo: depolarizing and hyperpolarizing components. J. Neurosci. 13 (8), 3252–3265.
Strauss, M., Sitt, J.D., King, J.R., Elbaz, M., Azizi, L., Buiatti, M., Naccache, L., van Wassenhove, V., Dehaene, S., 2015. Disruption of hierarchical predictive coding during sleep. Proc. Natl. Acad. Sci. U. S. A. 112 (11), E1353–E1362.
Todorovic, A., de Lange, F.P., 2012. Repetition suppression and expectation suppression are dissociable in time in early auditory evoked fields. J. Neurosci. 32 (39), 13389–13395.
Uhrig, L., Dehaene, S., Jarraya, B., 2014a. Cerebral mechanisms of general anesthesia. Ann. Fr. Anesth. Reanim. 33 (1), e15–e17.
Uhrig, L., Dehaene, S., Jarraya, B., 2014b. A hierarchy of responses to auditory regularities in the macaque brain. J. Neurosci. 34 (4), 1127–1132.
Umbricht, D., Schmid, L., Koller, R., Vollenweider, F.X., Hell, D., Javitt, D.C., 2000. Ketamine-induced deficits in auditory and visual context-dependent processing in healthy volunteers: implications for models of cognitive deficits in schizophrenia. Arch. Gen. Psychiatry 57 (12), 1139–1147.
Vanduffel, W., 2001. Visual motion processing investigated using contrast agent-enhanced fMRI in awake behaving monkeys. Neuron 32, 565–577.
Velly, L.J., Rey, M.F., Bruder, N.J., Gouvitsos, F.A., Witjas, T., Regis, J.M., Peragut, J.C., Gouin, F.M., 2007. Differential dynamic of action on cortical and subcortical structures of anesthetic agents during induction of anesthesia. Anesthesiology 107 (2), 202–212.
Vincent, J.L., Patel, G.H., Fox, M.D., Snyder, A.Z., Baker, J.T., Van Essen, D.C., Zempel, J.M., Snyder, L.H., Corbetta, M., Raichle, M.E., 2007. Intrinsic functional architecture in the anaesthetized monkey brain. Nature 447 (7140), 83–86.
Wacongne, C., Labyt, E., van Wassenhove, V., Bekinschtein, T., Naccache, L., Dehaene, S., 2011. Evidence for a hierarchy of predictions and prediction errors in human cortex. Proc. Natl. Acad. Sci. U. S. A. 108 (51), 20754–20759.
Wacongne, C., Changeux, J.P., Dehaene, S., 2012. A neuronal model of predictive coding accounting for the mismatch negativity. J. Neurosci. 32 (11), 3665–3678.
Ypparila, H., Karhu, J., Westeren-Punnonen, S., Musialowicz, T., Partanen, J., 2002. Evidence of auditory processing during postoperative propofol sedation. Clin. Neurophysiol. 113 (8), 1357–1364.